Contribution from the Department of Chemistry,
University of Pittsburgh, Pittsburgh, Pennsylvania 15260

Inner-Sphere Reduction of Dioxygen with the Binuclear Vanadium(III) Complex $V_2O(ttha)^{2-}$ and Studies of the $[V^{III},V^{IV}]$ Mixed-Oxidation-State Product

Terry K. Myser and Rex E. Shepherd*

Received January 24, 1986

Binuclear vanadium complexes of the triethylenetetraminehexaacetate ion, ttha^{6-}, have been studied in solution. The $[V^{III},V^{III}]$ complex is properly formulated as $V_2O(ttha)^{2-}$, having λ_{max} at 450 nm (LMCT, $\epsilon = 2.63 \times 10^3$ M^{-1} cm^{-1}/mol of V(III)) and 640 nm ($\epsilon = 260$ M^{-1} cm^{-1}/mol of V(III)). A reaction that is first order in both $[V_2O(ttha)^{2-}]$ and $[O_2]$ ($t_{1/2} \leq 11$ s) is observed to proceed by proton-independent and proton-assisted paths ($k_0 = 140$ M^{-1} s^{-1}, $k_1 = 2.08 \times 10^8$ M^{-2} s^{-1}). No free O_2^- or O_2^{2-} intermediates are detectable by enzyme (superoxide dismutase and catalase) or chemical scavenger tests and radical-trapping agents (DMPO, PBN). In the presence of excess O_2, an initial $[V^{III},V^{IV}O_2^-]$ intermediate is oxidized to $[V^{IV},V^{IV}]$ on a time scale of minutes. The slower complete oxidation may be intercepted by an Ar purge immediately after the rapid formation of the superoxo complex. $[V^{III},V^{IV}O_2^-]$ self-dismutes via a peroxo intermediate or is reduced rapidly to create a pool of the mixed-oxidation-state ttha^{6-} complex, $[V^{III},V^{IV}]$. Pairs of $[V^{III},V^{IV}]$ complexes execute a slow second-order cross-electron-transfer reaction, which generates the isovalent $[V^{III},V^{III}]$ and $[V^{IV},V^{IV}]$ species. The cross-reaction of $[V^{III},V^{IV}]$, as prepared via the superoxo complex, matches the rates of synthetic $[V^{III},V^{IV}]$ prepared by addition of 1:1:1 VCl_3:$VOSO_4$:ttha^{6-} at pH $\simeq$7.0. The cross-electron-transfer step has parallel proton-independent and first-order paths ($k_0^{cr} = (5.08 \pm 0.45) \times 10^{-2}$ M^{-1} s^{-1}; $k_1^{cr} = (6.53 \pm 0.68) \times 10^5$ M^{-2} s^{-1}). The comproportionation constant for formation of the mixed-oxidation-state $[V^{III},V^{IV}]$ complex from isovalent pairs is only 0.15 ± 0.04. Therefore, the isovalent species are favored by ca. 2.0 kcal/mol. The various binuclear vanadium species have been studied in solution by UV–vis, EPR, pH-titration, and differential pulse voltammetry methods.

Introduction

Polyamino polycarboxylic acids form a wide variety of stable water-soluble metal chelates with diverse properties and uses. Many of the homologous polyamino polycarboxylates of edta^{4-} are capable of forming mononuclear, binuclear, and even trinuclear metal chelate complexes. Triethylenetetraminehexaacetic acid was introduced by Frost.[1a] The anion form, ttha^{6-}, forms a number of binuclear complexes, particularly with labile first-row transition-metal ions.[1b] Binuclear complexes that have received study include the following: Fe(II), Fe(III);[2] Co(II), Cu(II), Ni(II);[3] Zn(II);[4] Cr(III);[5] Ti(III);[6] VO^{2+}.[7,8] ttha^{6-} has 10 possible coordination sites. The lability of metal centers coordinated to the framework of the ligand, together with varying degrees of protonation of the donor sites, makes structural assignments of the various equilibrium species a very difficult task. The concerns raised for the various structural isomers and protolytic forms are emphasized by the fact that known X-ray crystal structures for Cu(II) and VO^{2+} binuclear complexes are not compatible with their solution ESR data. Smith and Martell[3b] calculated a Cu(II)–Cu(II) distance of 5.5 Å on the basis of ESR data, and they concluded that a bridged Cu–X–Cu species would be required to account for the small distance. The X-ray analysis of Leverett[3c] on the solid $H_2Cu_2(ttha)\cdot H_2O$ reveals that the Cu(II) centers are fully extended in the lattice with a Cu–Cu distance of 7.655 Å. Similarly, the binuclear VO^{2+} complex of ttha^{6-} exhibits an extended structure with a vanadyl oxygen replacing the water ligand (shown by **1A** in Figure 1) and a VO–VO distance of 7.482 Å in the solid state;[8] yet the ESR spectrum of the solution species was observed to have a 15-line pattern by Smith, Boas, and Pilbrow.[9] These workers have concluded that a bridged complex related to structure **1B** is required to produce the 15-line pattern, as the extended-chain form at 7.48 Å is too remote to produce the required coupling; also an 8-line pattern would be observed for wholly separate VO^{2+} sites.[9] The present investigation includes an additional examination of the $[V^{IV},V^{IV}]$ binuclear complex of ttha^{6-} and data concerning the properties and reactivities of the $[V^{III},V^{III}]$ member of the series. The two complexes appear to retain a structural kinship in solution as well as with the related mixed-oxidation-state species $[V^{III},V^{IV}]$, which may be generated chemically by the reaction of O_2 with $[V^{III},V^{III}]$. Studies of these systems could provide some interesting insights into the chemistry of biometallic species such as hemerythrin or hemocyanin, where adjacent metal sites are held in the proper proximity by means of amino acid functional groups along a biopolymer backbone chain. The mechanism of the reaction between O_2 and $V_2O(ttha)^{2-}$, $[V^{III},V^{III}]$, is described here. In addition to its relationship with several biochemical O_2 carriers, this reaction is of potential importance for the reduction of O_2 in fuel cells where rapid electron transfer is needed at an O_2 cathode. The $V_2O(ttha)^{2-}/O_2$ reaction represents a possible alternative to the cofacial-porphyrin-designed catalysts.[24]

The nature of the mixed-oxidation-state species $[V^{III},V^{IV}]$ is of interest in its own right in relationship to other intervalent compounds such as the Creutz–Taube ion. Launay[10] and Saito[11] have recently described (pyridylmethyl)iminodiacetate complexes having a V_2O_3 core with one bridging oxo ligand. These systems show extensive delocalization of the $[V^{IV},V^{V}]$ species of this series. Launay et al. have estimated a comproportionation constant favoring the mixed-oxidation-state species of 10^{24}.[10a] Therefore, properties of related vanadium-containing intervalent ions in polyamino polycarboxylate environments are of particular interest in order to extend our understanding to systems other than the Creutz–Taube type.[26]

Experimental Section

Reagents. VCl_3 was synthesized from V_2O_5 and S_2Cl_2 according to the procedure of Brauer.[12] VCl_3 was also obtained from Alfa (Ventron

(1) (a) Frost, A. E. *Nature (London)* **1956**, *178*, 322. (b) Abbreviations: edta^{4-} = ethylenediaminetetraacetate; hedta^{3-} = *N*-(hydroxyethyl)-ethylenediaminetriacetate; ttha^{6-} = triethylenetetraminehexaacetate; PBN = *N*-*tert*-butyl-α-phenylnitrone; DMPO = 5,5′-dimethyl-1-pyrroline 1-oxide.

(2) (a) Bohigian, T. A.; Martell, A. E. *J. Inorg. Nucl. Chem.* **1967**, *29*, 453. (b) Myser, T.; Shepherd, R. E., to be submitted for publication in *Inorg. Chem.* (c) Schröder, K. H. *Acta Chem. Scand.* **1965**, *19*, 1797. (d) Harju, L.; Ringbom, A. *Anal. Chim. Acta* **1970**, *49*, 221. (e) Harju, L. *Anal. Chim. Acta* **1970**, *50*, 475.

(3) (a) Bohigian, T. A.; Martell, A. E. *Inorg. Chem.* **1965**, *4*, 1264. (b) Smith, T. D.; Martell, A. E. *J. Am. Chem. Soc.* **1972**, *94*, 4123. (c) Leverett, P. *J. Chem. Soc., Chem. Commun.* **1974**, 161.

(4) Kopanica, M.; Neubauer, L. *Collect. Czech. Chem. Commun.* **1971**, *36*, 1121.

(5) (a) Fallon, G. D.; Gatehouse, B. M. *Acta Crystallogr., Sect. B: Struct. Crystallogr. Cryst. Chem.* **1974**, *B30*, 1987. (b) Martinez, F. B.; Pena, A. L. *Acta Cient. Compostelana* **1971**, *8*, 85. (c) Smith, T. D.; Lancashire, R. J. *Aust. J. Chem.* **1975**, *28*, 2137.

(6) (a) Kristine, F. J. Ph.D. Thesis, University of Pittsburgh, 1980. (b) Cookson, D. J.; Smith, T. D.; Pilbrow, J. R. *J. Chem. Soc., Dalton Trans.* **1974**, 1396.

(7) Napoli, A. *Gazz. Chim. Ital.* **1976**, *106*, 597.

(8) Fallon, G. D.; Gatehouse, B. M. *Acta Crystallogr., Sect. B: Struct. Crystallogr. Cryst.* **1976**, *B32*, 71.

(9) Smith, T. D.; Boas, J. F.; Pilbrow, J. R. *Aust. J. Chem.* **1974**, *27*, 2535.

(10) (a) Launay, J.-P.; Jeannin, Y.; Daouidi, M. *Proc. Int. Conf. Coord. Chem., 23rd* **1984**, 482. (b) Babonneau, F.; Sanchez, C.; Livage, J.; Launay, J.-P; Daoudi, M.; Jeannin, Y. *Nouv. J. Chim.* **1982**, *6*, 353.

(11) (a) Nishizawa, N.; Hirotsu, K.; Ooi, S.; Saito, K. *J. Chem. Soc., Chem. Commun.* **1979**, 707. (b) Kojima, A.; Okazaki, K.; Ooi, S.; Saito, K. *Inorg. Chem.* **1983**, *22*, 1169.

0020-1669/87/1326-1544$01.50/0

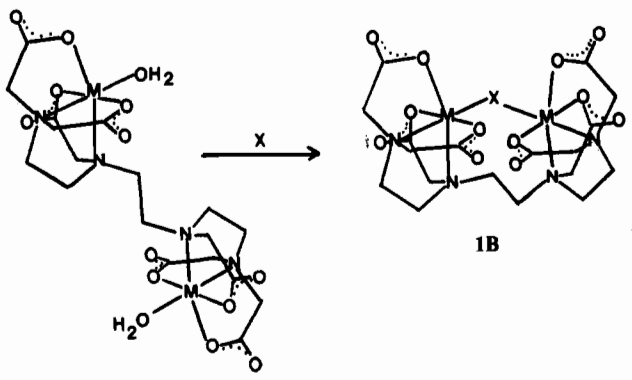

1A 1B

Figure 1.

Corp.) and Aldrich; $VOSO_4$ was supplied by Aldrich as the anhydrous solid. Triethylenetetraminehexaacetic acid, H_6ttha, was obtained from Sigma. DMPO and PBN radical traps[16] were obtained from Aldrich. The enzymes, bovine blood superoxide dismutase (SOD) and bovine liver catalase (CAT), were obtained from Sigma. These enzymes were maintained in the frozen state until immediately prior to use. Solutions were prepared at 0.10 ionic strength with NaCl and adjusted to near pH 7. O_2, N_2, and Ar gases were supplied by Air Products. N_2 and Ar gases, used to provide inert-atmosphere blanketing gases over the solutions having air sensitivity, were purified by passage through Cr(II) scrubbing towers followed by a H_2O rinse tower. Transfers of air-sensitive solutions were carried out by gastight syringe techniques, with stainless steel needles. O_2 solutions of desired concentrations were obtained by dilution of O_2-saturated solutions, which were prepared by bubbling an electrolyte solution maintained at 25.0 °C with O_2 for 1 h. Lower concentrations were obtained by syringe techniques transferring the O_2-saturated solution into an identical electrolyte solution that had been purged with N_2 or Ar at 25.0 °C.

UV–Visible Spectra. UV–visible spectral data were recorded on a Varian-Cary 118C spectrophotometer. Quartz cells were sealed with rubber septa and flushed with N_2 prior to filling with air-sensitive solutions.

Electrochemical Data. Vanadium complexes were examined by means of differential pulse voltammetry using an IBM-EC 225 analyzer. Saturated calomel and a platinum wire served as the reference and the auxiliary electrodes in a three-electrode assembly. The working electrode was either a glassy-carbon surface, polished with alumina, or a platinum-foil electrode. Calibration of the system was carried out with known reversible one-electron couples such as $Ru(NH_3)_6^{3+/2+}$, $Fe(CN)_6^{4-/3-}$, and $Fe(H_2O)_6^{3+/2+}$ (the last couple in 1 M $HClO_4$). Reference potentials are 0.051,[27a] 0.355,[27b] and 0.732 V,[27c] respectively.

$Na_2[V_2O(ttha)]$·dmf·$3H_2O$. A 2×10^{-3} mol amount of H_6ttha and 4×10^{-3} mol of VCl_3 were placed in a septum-sealed 100-mL three-necked round-bottom flask. The system was purged with N_2, and 15 mL of N_2-purged water was added. After the solution was stirred for 15 min, 6 M N_2-purged NaOH was added dropwise until the pH was between 7 and 8. The solution was heated at 75 °C for 2 h under a positive N_2 pressure. After it was cooled, the solution was suction-filtered in a glovebag under N_2 to remove any undissolved materials. The filtrate was transferred in the glovebag to a single-necked 100-mL round-bottom flask. Dimethylformamide, dmf, was added while the filtrate was cooled in an ice bath until precipitation was observed. The solid was collected on a glass frit. When the product appeared to be reasonably dry, the sample was transferred to a round-bottom flask and placed under vacuum to complete the solvent removal. Due to the air sensitivity of the solid, it was stored under vacuum. Elemental analysis (Galbraith Laboratories Inc.) of the product established the formula $Na_2[V_2O(ttha)]$·dmf·$3H_2O$. Anal. Found: C, 32.51; N, 9.16; H, 4.86. Calcd: C, 32.36; N, 8.99; H, 4.79.

Kinetic Studies. Kinetic data for the reaction between $V_2O(ttha)^{2-}$ and O_2 were collected on a Durrum D-110 stopped-flow spectrophotometer, interfaced with a DEC-1103 computer for data analysis. Data reduction and analysis was achieved by using appropriate first-order kinetic programs on floppy magnetic disks. Metal ion catalysis of the redox reactions was established early in certain studies. Immediately prior to use each day the flow path and cell compartment were flushed and soaked with a concentrated $edta^{4-}$ solution. After these parts were soaked for about 10 min to remove any reagents from other studies, the apparatus was thoroughly rinsed with doubly deionized water to remove the $edta^{4-}$ solution. Immediately prior to use of air-sensitive solutions the instrument was purged with N_2-saturated, doubly deionized water.

In spite of all the precautions taken, data collected from air-sensitive reactions were still complicated by O_2 leaks, which lowered the effective initial reagent concentration of the reducing solution. It was observed that oxidation of reducing reactants proceeds with the length of time the solution resides in the instrument. For example, successive runs of the reactions between $V_2O(ttha)^{2-}$ and O_2 had successively lower starting absorbances at a wavelength where $V_2O(ttha)^{2-}$ provides the absorbing species. The largest O_2 leaks seemed to be in the syringe and Teflon needle used to transfer solutions between the bubblers and the instrument. To minimize oxidation of reagents, the syringes were used strictly for making the transfer and not for storage of reagents as a reservoir for the drive syringe barrels as is customary for combining air-stable reactants in the stopped-flow device.

Lifetime studies of the mixed-oxidation-state $[V^{III},V^{IV}]$ complex were initially carried out by using a flow-cell assembly associated with the Varian-Cary 118C spectrophotometer. Chemical additions were achieved at a septum port of an electrochemical cell that contained 50–70 mL of reagent solution maintained at constant temperature via a flowing water jacket system. The internal cell solution was pumped by using a peristaltic pump through a 1.00-cm cell in the beam of the UV–visible spectrophotometer. Prior studies with dye solutions showed that the whole volume of the mixing cell, tubing, and observation cell is equilibrated in less than 30 s.

Pulse experiments were carried out by using an O_2 pulse to oxidize $[V^{III},V^{III}]$ to $[V^{III},V^{IV}]$ in the flow-cell assembly, followed by a purge with Ar. A cross reaction between two $[V^{III},V^{IV}]$ binuclear ions could then be monitored without competitive oxidation of the $[V^{III},V^{III}]$ product by O_2. This redox reaction was found to be very sensitive to the presence of trace contaminants such as Cu(II) or Fe(III). Cu(II), at levels present in analytical grade reagents, was found to catalytically oxidize the $[V^{III},V^{IV}O_2^-]$ intermediate, produced by the initial addition of O_2 to $[V^{III},V^{III}]$, unless the excess O_2 was removed by the Ar purge. In the stopped-flow experiment the influence of the slower catalytic oxidation was minimized by the Na_2H_2edta wash prior to each experiment. The occurrence of the slower catalytic oxidation step would not influence the measured stopped-flow rates because A_∞ was effectively zero for either the $[V^{III},V^{IV}O_2^-]$ species or its $[V^{IV},V^{IV}]$ derivative at the detection wavelength of 450 nm. Because of the difficulties in stopping the $[V^{III},V^{III}]$ oxidation at the $[V^{III},V^{IV}O_2^-]$ step in the flow-cell pulse O_2 experiments, the procedure was changed. Samples were prepared with Ar-purged solutions of $ttha^{6-}$ followed by addition of the requisite amounts of VCl_3 and/or $VOSO_4$. The O_2 reaction was initiated by injecting known volumes of O_2-saturated water. After bleaching of the $[V^{III},V^{III}]$ binuclear complex in about 1 min, any residual O_2 was removed by an Ar purge. Samples were taken by syringe techniques to obtain spectra in Ar-purged quartz cells. The $[V^{III},V^{IV}]$ ion was also prepared with 1:1:1 molar amounts of $ttha^{6-}$, VCl_3, and $VOSO_4$, respectively. Samples prepared in this manner allow for a theoretical check on the value of A_∞ because only half of the total moles will be recovered as the $[V^{III},V^{III}]$ ion (see the text). A_∞ can then be calculated from its value of $\epsilon_{450} = 2.63 \times 10^3$ M^{-1} cm^{-1}/mol of V(III). This scheme has the advantage that slow O_2 leaks, which would reduce the value of A_∞ from its correct value, will have much less impact on the kinetic studies. Second-order kinetic plots of $1/(A_\infty - A_t)$ vs. time for the initial rate region were constructed in the standard way by using least-squares fitting procedures with the DEC-1103 computer. Kinetic results obtained by the O_2 generation of $[V^{III},V^{IV}]$ from the $[V^{III},V^{III}]$ complex and by the direct formation of $[V^{III},V^{IV}]$ from weighed amounts of VCl_3 and $VOSO_4$ gave equivalent results.

Radical-Trapping Experiments. *N-tert*-Butyl-α-phenylnitrone (PBN) and 5,5-dimethyl-1-pyrroline *N*-oxide (DMPO) were employed. A stock solution of 3.0×10^{-2} M PBN was made by dissolving 0.053 86 g of PBN in 10.0 mL of deoxygenated water. A stock solution of 4.5×10^{-2} M DMPO was made by sampling 0.05 mL of DMPO with a gastight syringe in a glovebag under N_2 and then injecting the DMPO into 10.0 mL

(12) Brauer, G., Ed. *Handbook of Preparative Inorganic Chemistry*, 2nd ed.; Academic: New York, 1965; Vol. II, p 1256.
(13) (a) Shepherd, R. E.; Hatfield, W. E.; Ghosh, D.; Stout, C. D.; Kristine, F. J.; Ruble, J. R. *J. Am. Chem. Soc.* **1981**, *103*, 5511. (b) See references in ref 13a.
(14) Kristine, F. J.; Shepherd, R. E. *Inorg. Chem.* **1981**, *20*, 215.
(15) The formula $V_2O(ttha)^{2-}$ is established from the data of this report; 3.6 Å is a typical M–O–M distance for oxo-bridged first-row transition-metal complexes.
(16) Myser, T. K., unpublished work.
(17) Wieghardt, K.; Pohl, K.; Koeppen, M. *Proc. Int. Conf. Coord. Chem., 23rd* **1984**, 211.
(18) Johnson, C. R.; Shepherd, R. E. *Bioinorg. Chem.* **1978**, *8*, 115 and references therein.

of deoxygenated water in a bubbler on the Ar gas line. The PBN and DMPO solutions were stored under a continuous stream of Ar and transferred to the reaction mixtures by using gastight syringes. A stock solution of 3.0×10^{-3} M $V_2O(ttha)^{2-}$ at pH 7.4 was also stored under a continuous stream of Ar. For experiments involving H_2O_2 as the oxidizing agent the reaction mixtures were made by transferring 2.5 mL of the PBN or DMPO stock solutions to a deoxygenated solution of 1.0 mL of 3% H_2O_2 (and 0.5 mL of ethanol when appropriate). A 2.5-mL amount of $V_2O(ttha)^{2-}$ solution was added to the reaction mixture and immediately bleached. A portion of the reaction mixture was transferred to a deoxygenated flat quartz EPR cell, and the cell was mounted in the instrument. The manipulations required about 3 min. When O_2 was used as the oxidizing agent, the reaction mixture was made by combining appropriate amounts of $V_2O(ttha)^{2-}$, DMPO or PBN solution, and deoxygenated ethanol and water under an inert atmosphere. The reaction mixture was oxidized by bubbling a continuous stream of O_2 through the solution for 15 s followed by 2.5–3 min of vigorously bubbling Ar through the solution to purge excess O_2. A portion of the reaction mixture was transferred to the deoxygenated EPR cell and mounted in the instrument within 6 min of when O_2 was first introduced to the system.

pH Titration. Potentiometric titrations were carried out by using an Orion 701 pH meter with a combination glass/SCE minielectrode. Data for the titration curves were simultaneously recorded with a Fisher 5000 Recordall recorder electronically coupled with a Sage syringe pump. The syringe barrel was filled with standardized NaOH for titration of metal ion/ligand solutions, which were maintained in a thermostated cell, protected from the air with a blanket of N_2. The solutions were magnetically stirred, but continuous bubbling of N_2 through the solution also assured good mixing for titration work.

Results and Discussion

$[V^{III},V^{III}]$ Binuclear Ion. When V(III) is introduced at the two binding sites of $ttha^{6-}$, a spectrum of a pale purple species is found below pH 2.5. This species changes to a deep orange one, fully formed at pH 7.0. The stoichiometry of the V(III) complex was established by a mole ratio titration at 450 nm. At V(III):$ttha^{6-}$ ratios below 1.00 no feature in the spectrum in the region of 450 nm is similar to that of the binuclear complex as established in this work. The ϵ_{450} value for the mononuclear V^{III}/ttha complex is 22.9 at pH 7.5. When the V(III):$ttha^{6-}$ ratio is greater than 1.00, up to 2.00, the orange species is present. On the basis of V(III) as the limiting reagent, a constant ϵ value per mole of binuclear species is calculated, e.g. 5.26×10^3 M^{-1} cm^{-1}/2 mol of V(III). Above the ratio of 2.00 precipitation of a V(III) hydroxy species occurs. This shows that the $ttha^{6-}$ ligand will accommodate 2 mol of V(III)/mol of $ttha^{6-}$ as has been established previously for other first-row labile metal ions (Fe(II), Fe(III), Co(II), Cu(II), Ni(II), Zn(II), and VO^{2+}).[2-8] Beyond 2 mol of V(III)/mol of $ttha^{6-}$ the precipitation process shows that no stable 3:1 or higher complex forms. A solid of formula $Na_2[V_2O(ttha)]\cdot dmf\cdot 3H_2O$ was isolated as described in the Experimental Section. This compound also confirms the 2:1 stoichiometry. The orange binuclear V(III) complex was shown to be anionic by its absorption on AG1-4X anion-exchange resin in the Cl^- form but not on Dowex 50W-X8 cation-exchange resin in the Na^+ form. The orange complex was eluted rapidly from the AG1-4X resin with 4.0 M NaCl to avoid decomposition in the resin phase. The eluted ion gave a spectrum identical with that of the original solution. The binuclear complex therefore exhibits $\epsilon = 2.63 \times 10^3$ M^{-1} cm^{-1}/mol of V(III) at 450 nm and 260 M^{-1} cm^{-1}/mol of V(III) at 640 nm (see Figure 2).

The spectrum of the orange species differs from that of $[V(hedta\text{-}H)]_2$[13] and is more like that of $(hedta)Ti^{IV}OV^{III}(hedta)^-$ (λ_{max} = 453 nm, $\epsilon = 3.8 \times 10^2$ M^{-1} cm^{-1}).[14] Other oxo-bridged ions of related structure include the following: $[Fe_2O(hedta)_2]^{2-}$, λ_{max} = 477 nm, ϵ = 77 M^{-1} cm^{-1}/mol of Fe;[6] $Fe_2O(ttha)^{2-}$, λ_{max} = 477 nm, ϵ = 65 M^{-1} cm^{-1}/mol of Fe;[6] $(hedta)V^{II}OV^{IV}(hedta)^{2-}$, λ_{max} = 577 nm, $\epsilon = 1.36 \times 10^3$ M^{-1} cm^{-1}/2 mol of V.[19] The

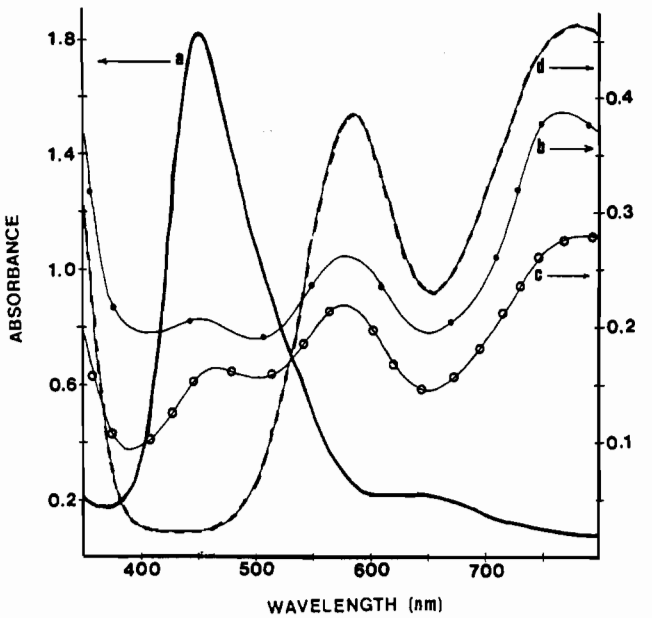

Figure 2. Visible spectra of binuclear vanadium–ttha Complexes: (a) $V_2O(ttha)^{2-}$ at pH 7.5, μ = 0.1, T = 25 °C, [V(III)] = 1.56×10^{-3} M, 1.0-cm cell, absorbance 0–2.0 (—); (b) products of $V_2O(ttha)^{2-}/O_2$ reaction, 1.0-cm cell, absorbance 0–0.5 (···); (c) $[V^{III},V^{IV}]$ at pH 6.5, [V(III)] = [V(IV)] = [$ttha^{6-}$] = 4.9×10^{-3} M, 2.0-cm cell, absorbance 0–0.5 (o); (d) $[V^{IV},V^{IV}]$ at pH 7.6, [V(IV)] = 1.2×10^{-3} M, [$ttha^{6-}$] = 0.6×10^{-2} M, 2.0-cm cell, absorbance 0–0.5 (- - -).

presence of a charge-transfer transition and titration data described below infer the formula $V_2O(ttha)^{2-}$. The orange color in the charge-transfer transition of $V_2O(ttha)^{2-}$ is bleached upon addition of phosphate or Tris buffer at constant pH. Since the minimum M–O–M distance is usually ca. 3.6 Å, the V–O–V unit in $V_2O(ttha)^{2-}$ should be strained.[15] We have observed that a buffer anion may rupture the strained V–O–V unit with proton transfer and binding of the buffer anion and OH^- on the V(III) centers.[6] This causes bleaching of the V^{III}–O^{2-}–V^{III} chromophore. In the absence of buffer ions, the spectrum at pH 7.0 remains constant.

A related case in which phosphate buffer catalyzes the opening of the chelate ring of $Ni(en)(H_2O)_4^{2+}$ was studied previously by Read and Margerum.[28] In the $Ni(en)(H_2O)_4^{2+}$/phosphate system the most active catalytic species is HPO_4^{2-} in spite of the fact that HPO_4^{2-} is a much poorer proton-transfer agent than $H_2PO_4^-$. The rupture of the $Ni(en)^{2+}$ chelate ring occurs by parallel general-acid-catalyzed pathways in which solvent H_2O, H_3O^+, H_3PO_4, $H_2PO_4^-$, and HPO_4^{2-} all play a significant role. The HPO_4^{2-} species has an electrostatic advantage in its attraction for $Ni(en)(H_2O)_4^{2+}$. Therefore, binding of the entering anion with Ni(II), together with proton transfer to the incipient, pendant $-CH_2CH_2NH_3^+$ unit, explains the kinetic advantage of HPO_4^{2-} toward the cationic $Ni(en)(H_2O)_4^{2+}$ complex.[28] In the case of

(19) Kristine, F. J.; Shepherd, R. E. *J. Am. Chem. Soc.* **1978**, *100*, 4398.
(20) Siddiqui, S.; Shepherd, R. E. *Inorg. Chem.* **1983**, *22*, 3726.
(21) (a) Fielden, E. M.; Roberts, P. B.; Bray, R. C.; Lowe, D. J.; Mautner, G. N.; Rotilio, G.; Calabrese, L. *Biochem. J.* **1974**, *139*, 49. (b) Fee, J. A. *Met. Ions Biol.* **1980**, *2*, 209–237.
(22) Kristine, F. J.; Shepherd, R. E. *Inorg. Chem.* **1981**, *20*, 2571.
(23) The formulation $TiO(edta)^{2-}$ applies to the solution species above pH ≅2. A solid isolated from a solution with pH ≅1 has the formula $Ti(edta)(H_2O)$. Its seven-coordinate structure has been determined: Fackler, J. P.; Kristine, F. J.; Mazany, A. M.; Moyer, T. J.; Shepherd, R. E. *Inorg. Chem.* **1985**, *24*, 1857. H_2O_2 reacts with $TiO(edta)^{2-}$, forming $Ti(O_2)(edta)^{2-}$; O_2^- will dismute to O_2 and O_2^{2-} and thus should also generate the orange $Ti(O_2)(edta)^{2-}$ complex if it were present.
(24) Durand, R. R.; Benscome, C. S.; Collman, J. P.; Anson, F. C. *J. Am. Chem. Soc.* **1983**, *105*, 2710.
(25) (a) Sharpe, A. G. *The Chemistry of Cyano Complexes of the Transition Metals*; Academic: New York, 1976; pp 179–181. (b) Haim, A.; Wilmarth, W. K. *J. Am. Chem. Soc.* **1961**, *83*, 509–516.
(26) (a) Creutz, C.; Taube, H. *J. Am. Chem. Soc.* **1973**, *95*, 1086–1094. (b) Creutz, C.; Taube, H. *J. Am. Chem. Soc.* **1969**, *91*, 3988–3989. (c) Lin, H. S.; Barclay, D. J.; Anson, F. C. *Inorg. Chem.* **1972**, *11*, 1460–1466.
(27) (a) Kuehn, C.; Taube, H. *J. Am. Chem. Soc.* **1976**, *98*, 689–702. (b) Hanania, G. I. H.; Irvine, D. H.; Eaton, W. A.; George, P. *J. Phys. Chem.* **1967**, *71*, 2022. (c) Skoog, D. A.; West, D. M. *Principles of Instrumental Analysis*; Holt, Rinehart and Winston: New York, 1971; pp 678–680.
(28) Read, R. A.; Margerum, D. W. *Inorg. Chem.* **1983**, *22*, 3447–3451.

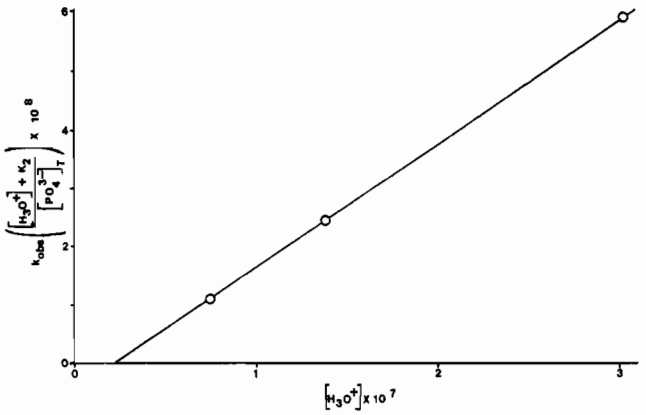

Figure 3. Hydrogen ion dependence of the charge-transfer bleaching of $V_2O(ttha)^{2-}$ by phosphate buffer (μ = 0.10 (phosphate species + NaCl); T = 21.0 °C; $[V_2O(ttha)^{2-}]_i = 8.135 \times 10^{-4}$ M; $[PO_4^{3-}]_{tot} = 4.63 \times 10^{-2}$ M).

$V_2O(ttha)^{2-}$ of this work, it was anticipated that the best proton donor of lowest anionic charge, e.g. $H_2PO_4^-$, would be the favored catalytic species to cause rupture of the strained V^{III}–O^{2-}–V^{III} chromophore. Since $V_2O(ttha)^{2-}$ is stable at pH 7.0 in the absence of phosphate buffer ions, the solvent-assisted and direct proton-catalyzed pathways must be negligible near pH 7.0 in the $V_2O(ttha)^{2-}$/phosphate bleaching reaction. Therefore in the pH range of 6.5–7.5, where the bleaching reaction is observed, one need only consider the major general-acid pathways, which involve $H_2PO_4^-$ and HPO_4^{2-} for ring rupture in $V_2O(ttha)^{2-}$. The bleaching reaction was first order in $[PO_4^{3-}]_{tot}$. Pseudo-first-order rate constants, k_B, for the bleaching process were measured at μ = 0.10 and T = 21.0 °C. The kinetic studies for phosphate-catalyzed ring opening of the V^{III}–O^{2-}–V^{III} chromophore were carried out with $[PO_4^{3-}]_{tot}$:$[V_2O(ttha)^{2-}] \geq 28$. Under these conditions only about 2.2% of $V_2O(ttha)^{2-}$ remains at infinite time as described below. The data, treated as $-\ln (A_\infty - A_t)$ with A_∞ taken as the 100% bleached value of the blank, gives a reliable value for k_B. The ionic strength was controlled by the sum of phosphate buffer species plus added NaCl electrolyte. Parallel paths for HPO_4^{2-} and $H_2PO_4^-$ catalysis require a hydrogen ion dependent rate constant as given by eq 1, where K_2 is the acid dissociation constant for $H_2PO_4^-$ and $[PO_4^{3-}]_{tot}$ is the total formal buffer concentration.

$$k_B = \frac{k_{H_2PO_4^-}[H_3O^+] + k_{HPO_4^{2-}}K_2}{[H_3O^+] + K_2}[PO_4^{3-}]_{tot} \quad (1)$$

A plot of the measured k_B rate constants treated as $k_B([H_3O^+] + K_2)/[PO_4^{3-}]_{tot}$ vs. $[H_3O^+]$ should be linear with slope of $k_{H_2PO_4^-}$ and intercept of $K_2k_{HPO_4^{2-}}$ if this general-acid scheme correctly describes the nature of the bleaching reaction in the $V_2O(ttha)^{2-}$/phosphate system. The appropriate plot is shown in Figure 3, with the literature value of 1.38×10^{-7} M^{-1} for K_2. Linearity is indeed observed with $k_{H_2PO_4^-} = 0.209 \pm 0.001$ M^{-1} s^{-1}. The intercept cannot be distinguished from zero. An upper limit for $K_2k_{HPO_4^{2-}}$ of 2.5×10^{-10} implies $k_{HPO_4^{2-}} \leq 1.8 \times 10^{-3}$. Therefore, the reactivity of HPO_4^{2-} is less than 0.9% of that found for $H_2PO_4^-$, as anticipated above. $H_2PO_4^-$ is approximately 6 times less efficient in promoting the V–O–V chromophore rupture than the $Ni(en)^{2+}$ chelate ring opening ($k_{H_2PO_4^-} = 0.209$ M^{-1} s^{-1} vs. 1.23 M^{-1} s^{-1} for $Ni(en)(H_2O)_4^{2+}$),[28] while $k_{HPO_4^{2-}}$ is at least 4 orders less efficient. This effect most likely resides in the addition of the $H_2PO_4^-$ or HPO_4^{2-} anions to anionic $V_2O(ttha)^{2-}$ compared to the cationic $Ni(en)(H_2O)_4^{2+}$ complex.

Although the first-order dependence in $H_2PO_4^-$ implicates $H_2PO_4^-$ as the general-acid active species and establishes that only 1 mol of $H_2PO_4^-$ is present in the transition state of the bleaching reaction, it remained to be established how many moles of $H_2PO_4^-$ are involved in the net equilibrium between $V_2O(ttha)^{2-}$ and $H_2PO_4^-$ (eq 2).

$$V_2O(ttha)^{2-} + nH_2PO_4^- \rightleftarrows [V_2O(ttha)(H_2PO_4)_n^{n+2}] \quad (2)$$

Table I. Equilibrium Studies of the $H_2PO_4^-/V_2O(ttha)^{2-}$ Interaction[a]

	trial				
	1	2	3	4	5
$[H_2PO_4^-]/[V_2O(ttha)^{2-}]_i$	3.14	5.00	6.25	7.50	9.38
$10^4[V_2O(ttha)^{2-}]_f = C$, M	1.89	1.02	0.808	0.783	0.582
$10^3[P] = C_0 - C$, M	1.80	1.89	1.91	1.91	1.93
$10^2[H_2PO_4^{2-}]$, M	0.625	1.00	1.25	1.50	1.875
$10^{-3}K$ for n = 1	1.52	1.85	1.89	1.63	1.77
$10^{-5}K$ for n = 2	2.44	1.85	1.51	1.08	0.94

[a] Conditions: μ = 0.10 (phosphate + added NaCl); pH 6.86; T = 21.0 °C; $[V_2O(ttha)^{2-}]_i = 1.99 \times 10^{-3}$ M = C_0.

It was observed at low ratios of $[PO_4^{3-}]_{tot}$:$[V_2O(ttha)^{2-}]$ between 2.0 and 9.5 that the bleaching process reaches an equilibrium in which a spectrophotometrically detectable amount of $V_2O(ttha)^{2-}$ remains rather than 100% formation of the bleached product. About 12 h was required to achieve equilibrium, as shown by a constant final absorbance, monitored at 450 nm. The equilibrium constant describing eq 2 was treated by eq 3, where the bleached

$$K = \frac{[P]}{[V_2O(ttha)^{2-}]_f[H_2PO_4^-]^n} \quad (3)$$

reaction product concentration, [P], equals the total initial $[V_2O(ttha)^{2-}]_i$ minus $[V_2O(ttha)^{2-}]_f$ at equilibrium. The equilibrium constant (eq 3) was calculated for experimental data at ratios from 3.14 to 9.38 with n = 1 and n = 2. Data shown in Table I were obtained at 21.0 °C, μ = 0.10 (phosphate + NaCl), and a constant pH of 6.86. The experiments gave average values for K of $(1.7 \pm 0.1) \times 10^3$ M^{-1} for n = 1 and $(1.6 \pm 0.9) \times 10^5$ M^{-2} for n = 2. The significantly larger error (56% with n = 2 vs. 12% for n = 1) and spread in the values calculated for K under different ratios of buffer:$V_2O(ttha)^{2-}$ argues for the value of n = 1 in eq 2 and 3. Assuming n = 1, $V_2O(ttha)^{2-}$ reacts with $H_2PO_4^-$ to form one V(III) center bound by OH^- and the other bound by HPO_4^{2-}. The condition must involve rupture of the oxo bridge as the charge-transfer band is bleached. Opening of another chelate ring such as a coordinated carboxylate would not alter the charge-transfer absorption appreciably.

$[V^{III},V^{IV}]$ Binuclear Ion. Attempts to isolate Na^+, Ca^{2+}, etc. salts of $V_2O(ttha)^{2-}$ have shown the species to be very air-sensitive. Only $Na_2[V_2O(ttha)]$·dmf·$3H_2O$ was successfully isolated. In solution, the reaction with O_2 occurs within seconds. Parallel studies on monomeric V(hedta)(H_2O) show that the oxidation is slow, requiring 17 h in saturated O_2 solution to approach completion. $[V(hedta\text{-}H)]_2^{2-}$ requires about 5 min for complete oxidation.[16] Clearly differences in reactivity exist for monomeric V(III) vs. the binuclear cases. The sided molecule[43] $V_2O(ttha)^{2-}$ reacts more rapidly than the protected binuclear one,[13] $[V(hedta\text{-}H)]_2^{2-}$. The autoxidation product of V(hedta)(H_2O) or $[V(hedta\text{-}H)]_2^{2-}$ is $VO(hedta)^-$. In contrast $V_2O(ttha)^{2-}$ reacts with O_2 to form a $[V^{III},V^{IV}]$ complex (see curve c, Figure 2).

The $[V^{III},V^{IV}]$ ion exhibits bands characteristic of both a V(IV) site (~765 nm, ϵ = 27.0 ± 2.0 M^{-1} cm^{-1}; 580 nm, ϵ = 19.5 ± 2.9 M^{-1} cm^{-1}) and a V(III) site (450 nm, ϵ = 14.9 ± 1.4 M^{-1} cm^{-1}). It is impossible to eliminate contributions of $[V^{III},V^{III}]$ and $[V^{IV},V^{IV}]$ to the spectrum, however. This is due to the fact that $[V^{III},V^{IV}]$ undergoes a cross-electron-transfer reaction on a slow time scale to generate $[V^{III},V^{III}]$ and $[V^{IV},V^{IV}]$. This process is described in a later section.

Parallel titration data were obtained for titratable protons through pH 10 in the formation of $[V^{IV},V^{IV}]$, $[V^{III},V^{IV}]$, and $[V^{III},V^{III}]$. $[V^{IV},V^{IV}]$ consumed 6 protons,[7,8] while $[V^{III},V^{IV}]$ consumed 7.0 ± 0.1 and $[V^{III},V^{III}]$ consumed 8.0 ± 0.1. Methods are described in the Experimental Section, and the observed titration curves are shown in Figure 4. The formulation of the $[V^{III},V^{III}]$ complex as $V_2O(ttha)^{2-}$ is compatible with 6 protons from H_6ttha plus 2 protons from H_2O in forming the bridging oxo group; the latter group is also implicated by the intense charge-transfer transition at 450 nm.

Nature of the $[V^{IV},V^{IV}]$ Complex. The solution ESR spectra of $VO(ttha)^{4-}$ and $VO(hedta)^-$ at 298 K are nearly identical as

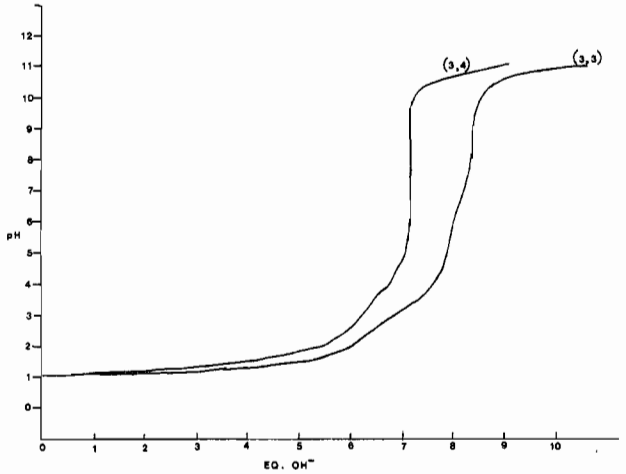

Figure 4. Potentiometric titration of $[V^{III},V^{III}]$ and $[V^{III},V^{IV}]$ binuclear complexes with NaOH (μ = 0.10; T = 21.0 °C; $[V^{III},V^{III}]$ = 1.00 × 10^{-3} M; $[V^{III},V^{IV}]$ = 1.00 × 10^{-3} M; [NaOH titrant] = 1.00 M).

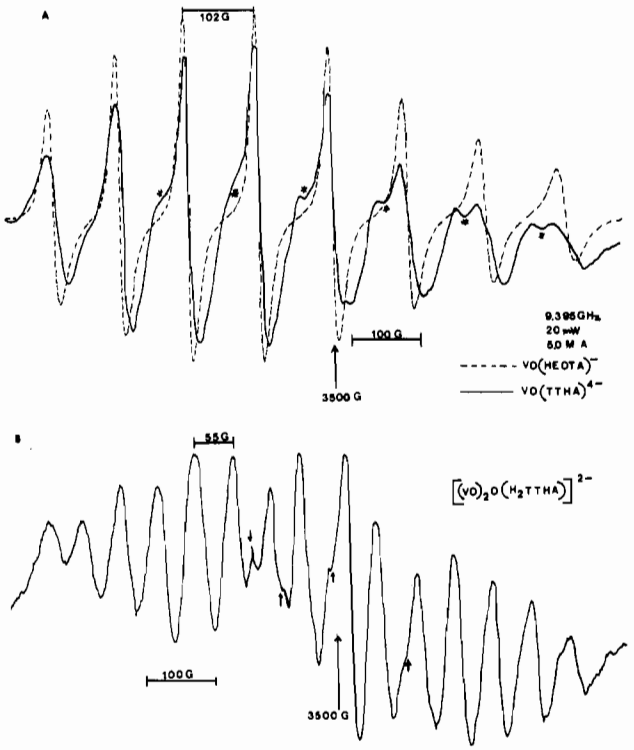

Figure 5. Room-temperature ESR spectra of vanadium(IV) complexes: (A) $[VO(hedta)^-]$ = 0.010 M, $[VO(ttha)^{4-}]$ = 0.010 M; (B) $[(VO)_2O(H_2ttha)^{2-}]$ = 0.005 M. All spectra were obtained in a flat quartz cell at 9.395 GHz, 20-mW power, and 5.0-G modulation amplitude; receiver gains (A) 1.25 × 10^3 and (B) 2.0 × 10^4.

shown in Figure 5A. Spin Hamiltonian parameters for the pair are observed to give A_{iso} = 102 G and g = 1.96. The first-derivative spectrum of $VO(ttha)^{4-}$ shows a trace equilibrium amount of the $[V^{IV},V^{IV}]$ binuclear ion, which produces distortions at positions indicated by asterisks in the figure. The $[V^{IV},V^{IV}]$ complex exhibits the spectrum shown in Figure 5B. Trace amounts of the equilibrium monosubstituted $VO(ttha)^{4-}$ cause distortions of the first-derivative spectrum at positions marked by arrows in Figure 5B. Spin Hamiltonian values are A_{iso} = 55 G and g = 1.96 for $[V^{IV},V^{IV}]$. The ESR spectrum of the $[V^{IV},V^{IV}]$ complex confirmed the result of Smith, Boas, and Pilbrow.[9] We observed the same 15-line pattern, which was insensitive to dilution to the limit of obtaining a resolved spectrum about g = 2. The coupling for A_{iso} suggests a V–V separation of 3.0–3.6 Å.[9] We measured the magnetic moment by the Evans method at 305 K. The μ_B value per V(IV) was found to be 1.51 instead of 1.73 for an uncoupled d^1 site. The UV–visible spectrum is shown in curve

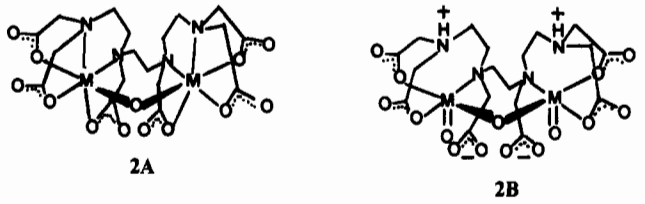

2A **2B**

Figure 6.

d of Figure 2. The titration data for formation of $[V^{IV},V^{IV}]$ implicates consumption of only 6 protons, yet the existence of oxo (or dihydroxy) bridging between V(IV) centers in solution is necessary to account for the ESR spectrum. The titration data reported here confirm the results of Napoli[7] and Smith et al.[9] for the formation of $[V^{IV},V^{IV}]$. Wieghardt et al. have reported a bis(μ-hydroxy)-bridged cationic complex of vanadyl centers, $[VO(9\text{-ane}N_3)OH]_2^{2+}$.[17] We favor the oxo-bridged species to explain the solution chemistry of $[V^{IV},V^{IV}]$. The $[V^{III},V^{III}]$ complex has the structure **2A** shown in Figure 6, which contains the strained oxo-bridging unit. V(IV) in polyamino polycarboxylate complexes such as $VO(edta)^{2-}$ shows a marked preference for pseudo-square-pyramidal coordination with labile positions trans to the oxo group of VO^{2+}.[18] If $[V^{IV},V^{IV}]$ were to adopt the structure shown by **2A** in Figure 6, the protons would reside on the most basic sites in the molecule, existent through pH 9. The structural conversion to the $[V^{III},V^{IV}]$ complex could be easily achieved with minimum rearrangement by removal of a proton and coordination of one of the axial amine nitrogens during a 1e reduction of $[V^{IV},V^{IV}]$. By this path, formation of $[V^{III},V^{IV}]$ is consistent with 7 protons titrated in forming $[V^{III},V^{IV}]$ in the potentiometric titration study. Other data relevant to the structure of $[V^{III},V^{IV}]$ to the extent of bridging in this complex have been elusive due to the inherent reactivity of this ion as described in the next section.

Cross-Electron-Transfer Reaction of $[V^{III},V^{IV}]$. Preparation of the mixed-oxidation-state $[V^{III},V^{IV}]$ complex was achieved by two methods. $[V^{III},V^{III}]$ is oxidized by O_2 to yield the $[V^{III},V^{IV}]$ ion. This process involves a series of reactions that are described in later sections. The same $[V^{III},V^{IV}]$ ion can be generated directly from equimolar amounts of VCl_3, $VOSO_4$, and $ttha^{6-}$ at a pH between 7 and 8. VCl_3 and $VOSO_4$ are added simultaneously to an Ar-purged solution of the $ttha^{6-}$ ligand. Substitution of V(III) and V(IV) occurs to give a kinetically determined mixture of the $[V^{III},V^{IV}]$, $[V^{III},V^{III}]$, and $[V^{IV},V^{IV}]$ in a ratio that differs from the statistical 2:1:1. A representative run exhibits a kinetic split such that $[V^{III},V^{IV}]$, $[V^{III},V^{III}]$ and $[V^{IV},V^{IV}]$ are produced in a ratio nearer to 3:1:1. Repetitive spectra from 700 to 350 nm were taken at suitable intervals for 3 h. The cross-electron-transfer reaction (eq 4) was observed by the increase in the spectral features

$$2[V^{III},V^{IV}] \xrightarrow{k^{cr}} [V^{III},V^{III}] + [V^{IV},V^{IV}] \qquad (4)$$

of the more absorbing $[V^{III},V^{III}]$ ion. A dissociative interchange of metal ions can be ruled out since the reaction progress is not first order in $[V^{III},V^{IV}]$. Furthermore, independent studies of various binuclear ions in the presence of small amounts of V(III) and V(IV) free metal ions at this pH show no increase in the rate of formation of $[V^{III},V^{III}]$ or $[V^{IV},V^{IV}]$ on even much longer time scales. The reaction progress, for kinetic purposes, was followed for the first 3 h; the reaction, depending on the pH, was complete in ca. 10–12 h. The theoretical value of A_∞ based on the initial amount of V(III) was used in the kinetic plots. Thus at A_∞, half of the total vanadium is the $[V^{III},V^{III}]$ complex. The value of A_{450} at any time t exhibits a second-order dependence as shown in Figure 7. The sensitivity of the second-order rate constant (k^{cr}) as a function of pH was studied. The data in Figure 8 reveal k^{cr} to be composed of a second-order constant, independent of $[H_3O^+]$, and a third-order constant that is first-order in $[H_3O^+]$ (eq 5).

$$k^{cr} = k_0^{cr} + k_1^{cr}[H_3O^+] \qquad (5)$$

The values of k_0^{cr} = (5.08 ± 0.45) × 10^{-2} M^{-1} s^{-1} and k_1^{cr} = (6.53

Table II. Differential Pulse Data for Vanadium–Polyamino Polycarboxylate Complexes[a]

species	assigned change	glassy carbon[b] vs. SCE, V	Pt[b] vs. SCE, V
$V^{III}_2(ttha) = V_2O(ttha)^{2-}$	III → IV either slow, fast 1e or simultaneous 2e	0.850	0.890
	IV → V	0.975	1.020
$V^{III},V^{IV}(ttha) = [V(O)VO(Httha)]^{2-}$	III → IV	0.840	0.850
	IV → V	0.980	1.020
$V^{IV}_2(ttha) = [(VO)_2O(H_2ttha)]^{2-}$	IV → V	0.980	1.030
$V^{IV},V^{V}(ttha)$	IV → V		1.000
$V^{III}(ttha)^{3-}$ (monomer)	III → IV	0.870	0.880
	IV → V	0.960	1.000
$V(hedta)(H_2O)$	III → IV	0.740	0.700
	IV → V	0.960	0.955
$[V(hedta\text{-}H)]_2^{2-}$	III → IV	0.470	0.470
	IV → V	0.930	0.955
$V^{IV}O(hedta)^-$	IV → V	0.930	0.960

[a] Conditions: T = 25.0 °C; μ = 0.10 (NaCl); peak widths ca. 90 mV. [b] Nonthermodynamic reduction potential vs. SCE.

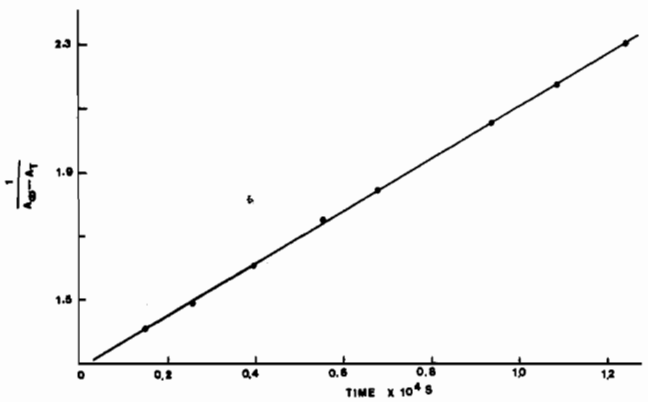

Figure 7. Representative second-order plot of the cross-electron-transfer reaction of $[V^{III},V^{IV}]$ ($[V(III)] = [V(IV)] = [ttha^{6-}] = 3.8 \times 10^{-3}$ M; T = 20 °C; μ = 0.05).

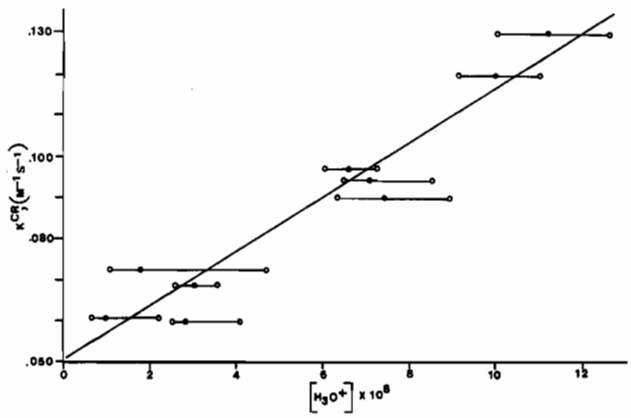

Figure 8. Hydrogen ion dependence of the cross-electron-transfer reaction of $[V^{III},V^{IV}]$ (T = 20 °C; μ = 0.05). Solid circles indicate the most stable $[H_3O^+]$ during the course of each run. Open circles indicate the minimum and maximum $[H_3O^+]$ during the course of the runs.

$\pm$ 0.68) $\times 10^5$ M^{-2} s^{-1} were determined from the most stable estimate of $[H_3O^+]$ during the reaction (solid circles). As the pH is near 7, the drift in unbuffered solutions was a problem, perhaps due to slight O_2 leaks, which would consume H_3O^+. pH data were taken throughout the course of the cross reaction, and the maximum and minimum values of $[H_3O^+]$ are shown by the range in the open circle points. If their mean value is used to define k_0^{cr} and k_1^{cr}, nearly equivalent results were obtained: $k_0^{cr} = (5.03 \pm 0.46) \times 10^{-2}$ M^{-1} s^{-1}; $k_1^{cr} = (6.25 \pm 0.66) \times 10^5$ M^{-2} s^{-1}. Protonation of a carboxylate cis to the N donor at the V(III) site might have a preequilibrium association constant k_H^{cr} as large as 10^2 while the N donor, itself, might have a K^{cr}_H value of about 10^5. These estimates are made on the basis of the pK_a's of the typical RCOOH and R_3NH^+ acids by assuming that the presence of the 3+ charge of V(III) should lower the affinities of the conjugate base forms by about 10^3 for anions and at least 10^5 for neutrals. The constant k_1^{cr} would be the product of a preequilibrium association of H^+ for the $[V^{III},V^{IV}]$ complex, k_H^{cr}, and its second-order electron-transfer rate k_{et}^{cr}. Therefore, k_{et}^{cr} will be either ca. 6.53×10^3 or 6.53 M^{-1} s^{-1} depending on whether the site of protonation is at the carboxylate or the N-donor which is trans to the bridging oxo ligand. Protonation at either of these positions would facilitate the necessary structural change compatible with the structure of the $[V^{IV},V^{IV}]$ complex, a product of the cross reaction. The unassisted path has the electron-transfer rate constant of 5.08×10^{-2} M^{-1} s^{-1}. The proton-assisted path has a relative advantage for k_{et}^{cr} of about 1.3×10^5 if protonation is at the leaving glycinate–carboxyl group and 128 if protonation is at the N-donor group.

Assessment of the Comproportionation Constant. Solutions of the synthetically prepared $[V^{III},V^{IV}]$ complex reach equilibrium through the cross reaction after about 13.5 h. The value of the comproportionation constant, K_{com}, $[V^{III},V^{III}] + [V^{IV},V^{IV}] \rightleftarrows 2[V^{III},V^{IV}]$ was found to be 0.15 $\pm$ 0.04 by spectrophotometric determination of the final amount of $[V^{III},V^{III}]$ and the total [V(III)] present. A statistical distribution gives K_{com} = 4.0. Thus in this case the isovalent complexes are modestly more stable than the mixed-oxidation-state binuclear ion, compared to the reverse situation for the Creutz–Taube ion, where $K_{com} \cong 6.0 \times 10^6$.[26] Expressed in the direction of a net favorable reaction ($2[V^{III},V^{IV}] \rightarrow [V^{III},V^{III}] + [V^{IV},V^{IV}]$), $k^* = 6.7 \pm 2.3$ with a statistical constant of 0.25. K_{com} is generally corrected for comparison with the statistical value by calculating K_{com}/K_{stat}. In the current study $K^*_{cor} \cong 6.7/0.25 \cong 27$. The extra stability probably originates largely in delocalization of the $[V^{III},V^{III}]$ complex since this complex is more resistant to loss of the first electron electrochemically; the extra stability is about 2.0 kcal/mol. This is only a slight factor of 2 higher than the $(bpy)_2ClRu^{II}pzRu^{III}(bpy)_2Cl^{3+}$ prepared by Meyer et al. but very much lower than the K_{cor} value of 10^{24} for the V(IV)–V(V) delocalization in the (pyridylmethyl)iminodiacetate complexes studied by Launay and Saito.[10,11] The rate of the reaction between $[V^{III},V^{III}]$ and $[V^{IV},V^{IV}]$ may be calculated from $K^* = 6.7$ and the cross-electron-transfer rate constant, k_{obsd} = 0.125 M^{-1} s^{-1}, yielding 1.9×10^{-2} M^{-1} s^{-1}.

Electrochemical Behavior of Binuclear Complexes. No reversible electrochemical waves are found for the binuclear ions on the cyclic voltammetric time scale at Pt or glassy carbon. Data in Table II where obtained by differential pulse voltammetry. Virtually equivalent results were obtained throughout the range of 2–15 mV/s in sweep rate or 10–75 mV for the pulse amplitude; the best data for Table II were obtained at 5 mV/s and a step of 50 mV for the pulse amplitude. Peak widths were ca. 90 mV, which

implicate some irreversibility.[29] The slower time scale of the differential pulse method allows for electrochemical events that follow slow processes, such as a chelate ligand reorganization, to be detected. The $[V^{III},V^{III}]$ complex is more difficult to oxidize than would be predicted from its monomer V^{III}–ttha complex (0.850 V vs. a predicted 0.834 V); it is also 10 mV harder to oxidize than the $[V^{III},V^{IV}]$ ion at glassy carbon. The electrochemical behavior of $[V^{IV},V^{IV}]$ is similar to that of mononuclear V(IV) complexes. The assigned changes in oxidation state for the complexes in Table II are based on the similarity of the IV → V oxidations for the authentic V(IV) monomer complexes. These waves are in the same potential region as the last oxidation wave observed for the binuclear ions and match the wave observed for the $[V^{IV},V^{IV}]$ ion.

The potentials that are observed for the various vanadium complexes of $ttha^{6-}$ and $hedta^{3+}$ in Table II must be nonthermodynamic potentials that are shifted from the thermodynamic value by a kinetic overvoltage.[29] O_2 readily oxidizes $[V^{III},V^{III}]$ in solution; however, the potential found at glassy carbon would predict that this would not be so. In solution $[V^{III},V^{III}]$ is readily oxidized by a number of outer-sphere one-electron oxidants including $Ru(NH_3)_6^{3+}$, $Ru(NH_3)_5Cl^{2+}$, $Ru(en)_3^{3+}$, $Fe(ox)_3^{3-}$, $Fe(CN)_6^{3-}$, and $IrCl_6^{2-}$. Therefore, the true potentials, unimpeded by a kinetic overvoltage at an electrode surface, must be significantly lower than those in Table II. The difference between the solution and electrochemical oxidations is due to several factors: (i) The change in oxidation state between V(III) and V(IV) occurs with a change in coordination number leading to slow electron transfer. (ii) Electrochemically $[V^{III},V^{IV}]$ is more readily oxidized than $[V^{III},V^{III}]$—thus assuring a net $2e^-$ change at a given potential suitable to oxidize $[V^{III},V^{III}]$ at the electrode surface, while solution chemistry may occur by $1e^-$ sequential events. (iii) In the chemical oxidation, as by O_2, additional driving force can be obtained from sequential reduction steps with O_2^-, O_2^{2-}, etc. and/or by binding of a substrate, such as O_2. Therefore, the data in Table II may be used only as a diagnostic indicator of the oxidation-state level for each species and as an approximate ranking of electrochemical reactivity. One may conclude that $[V(hedta\text{-}H)]_2^{2-}$ is more electron-rich as a dianion and is more reducing than V(hedta)(H_2O), a neutral species. $[V(hedta\text{-}H)]_2^{2-}$ is much more readily oxidized than $V_2O(ttha)^{2-}$. The bridging is by two alkoxy groups,[13] with weak V(III)–V(III) coupling, in $[V(hedta\text{-}H)]_2^{2-}$, while that of $V_2O(ttha)^{2-}$ is the oxo bridge. It is anticipated that greater vanadium–vanadium interaction occurs for the oxo bridge.[13b] This appears to be implicated in the first oxidation step for each complex. $[V(hedta\text{-}H)]_2^{2-}$ loses an electron much easier, by ca. 0.42 V, than $V_2O(ttha)^{2-}$; however, the meaning is obscured by possible differences in the kinetic overvoltages of the different complexes.

Kinetics of the $O_2/V_2O(ttha)^{2-}$ Reaction. The reaction between $V_2O(ttha)^{2-}$ and excess O_2 was studied by stopped-flow techniques under pseudo-first-order conditions. In most experiments the initial $[O_2]$ was 6.25×10^{-4} M (saturated O_2 solution) and the initial $[V_2O(ttha)^{2-}]$ was 2.34×10^{-4} M ($\mu = 0.10$, $T = 25.0$ °C). The visible spectrum indicated that $V_2O(ttha)^{2-}$ is oxidized by a net amount of one electron to the $[V^{III},V^{IV}]$ complex. The progress of the reaction was followed by the decay of the 450-nm maximum for $V_2O(ttha)^{2-}$. An exponential change for the A_{450} value indicated a first-order dependence on $[V_2O(ttha)^{2-}]$. $[O_2]$ at half the 6.25×10^{-4} M level reduced the rate by half, showing the rate law to be first order in $[O_2]$. A plot of the observed second-order rate constant as a function of $[H_3O^+]$ is shown in Figure 9. The linear dependence on $[H_3O^+]$ with a positive intercept indicates

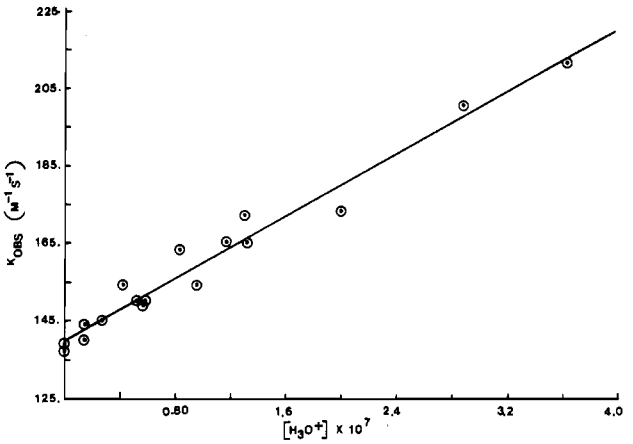

Figure 9. Hydrogen ion dependence of the $V_2O(ttha)^{2-}/O_2$ reaction ($T = 25.0$ °C; $\mu = 0.10$).

the overal rate law for the $V_2O(ttha)^{2-}/O_2$ reaction is as in eq 6. The values of k_0 and k_1 are $k_0 = 140$ M^{-1} s^{-1} and $k_1 = 2.08 \times 10^8$ M^{-2} s^{-1}. In the presence of traces of Cu(II), the reaction of O_2 and $V_2O(ttha)^{2-}$ is greatly accelerated and the product is $[V^{IV},V^{IV}]$. It was necessary to follow the careful washing procedure with $edta^{4-}$ solution as described in the Experimental Section in order to avoid the influence of Cu(II), which was present in the stopped-flow apparatus due to other kinetic work being pursued independently in our laboratory[20] at the time of our $V_2O(ttha)^{2-}/O_2$ experiments.

$$\frac{-d[V_2O(ttha)^{2-}]}{dt} = (k_0 + k_1[H_3O^+])[V_2O(ttha)^{2-}][O_2] \quad (6)$$

Free superoxide and peroxide might be intermediates in the reaction of $V_2O(ttha)^{2-}$ and O_2. If free superoxide anion is produced in the rate-determining step and then reduced to water in subsequent reactions, the reaction proceeds as follows with $k_{obsd} = 4k_m$:

$$V_2O(ttha)^{2-} + O_2 \xrightarrow{k_m} V^{III}V^{IV}(ttha) + O_2^- \quad (7)$$

$$O_2^- + 3V_2O(ttha)^{2-} \xrightarrow{4H^+} 3V^{III}V^{IV}(ttha) + 2H_2O \quad (8)$$

$$\text{net: } 4V_2O(ttha)^{2-} + O_2 \xrightarrow{4H^+} 4V^{III}V^{IV}(ttha) + 2H_2O \quad (9)$$

$$\text{rate} = -\frac{d[V_2O(ttha)^{2-}]}{dt} = \frac{d[V^{III}V^{IV}(ttha)]}{dt} = 4k_m[V_2O(ttha)^{2-}][O_2] \quad (10)$$

Superoxide dismutase is an enzyme that catalyzes the dismutation of superoxide into peroxide and oxygen. This dismutation reaction proceeds at a rate close to the diffusion limit ($\sim 2 \times 10^9$ M^{-1} s^{-1}).[21] Assuming the dismutation reaction is faster than the reaction between O_2^- and $V_2O(ttha)^{2-}$, the rate may be calculated as $2k_m$ in the presence of superoxide dismutase if O_2^- were formed in outer sphere (eq 13). The two calculations show that the reaction rate

$$V_2O(ttha)^{2-} + O_2 \xrightarrow{k_m} V^{III}V^{IV}(ttha) + O_2^- \quad (7)$$

$$O_2^- \xrightarrow{SOD} {}^1/_2O_2^{2-} + {}^1/_2O_2 \quad (11)$$

$$V_2O(ttha)^{2-} + {}^1/_2O_2^{2-} \xrightarrow{2H^+} V^{III}V^{IV}(ttha) + H_2O \quad (12)$$

$$\text{rate} = -\frac{d[V_2O(ttha)^{2-}]}{dt} = \frac{d[V^{III}V^{IV}(ttha)]}{dt} = 2k_m[V_2O(ttha)^{2-}][O_2] \quad (13)$$

should be cut in half by the addition of superoxide dismutase. When superoxide dismutase was added to the $V_2O(ttha)^{2-}/O_2$ system at $[SOD] = 1.08 \times 10^{-5}$ M, no appreciable change in the rate was observed. The rate observed was $(9.6 \pm 0.9) \times 10^{-2}$ s^{-1} without the enzyme and 8.8×10^{-2} s^{-1} with the enzyme. These

(29) A reviewer has suggested the use of chemical mediators to overcome the kinetic barriers at the electrode surface. Specifically, the use of $Ru(NH_3)_6^{2+/3+}$ was suggested as the logical mediator. However, experiments conducted in our laboratory even prior to the reviewer's suggestion had shown that the presence of $Ru(NH_3)_6^{2+}$ provides a pathway to alternate bridged L^{IV}–O–$Ru^{II}(NH_3)_5$ species related to those characterized previously in our laboratory: Kristine, F. J.; Shepherd, R. E. *Inorg. Chem.* **1978**, *17*, 3145–3152. These results will be described in a future publication.

numbers are within the range of normal experimental variance for the reaction conditions. Under these conditions at least a 50% kinetic split in any O_2^- formed via an outer-sphere path would occur even if the rate constant in eq 8 were as large as 9.2×10^7 M^{-1} s^{-1}. A significant rate reduction would be seen even if as much as 10% of any O_2^- were trapped competitively by the SOD enzyme and if eq 8 were to proceed at the diffusion limit. Direct radical-trapping studies for free O_2^- described in a subsequent section substantiate that no outer-sphere production of O_2^- is contributory to the $V_2O(ttha)^{2-}/O_2$ redox process in any amount greater than 12.5%. Thus the major pathway does not involve free O_2^- and SOD has no effect.

Alternately, the rate-determining step may involve the production of free peroxide instead of superoxide. The enzyme, catalase, scavenges peroxide ion at a rapid rate and could be used in the same manner as superoxide dismutase. The relative reaction rates can be calculated with and without catalase added; again $4k_m'$ and $2k_m'$, respectively:

with no enzyme

$$2V_2O(ttha)^{2-} + O_2 \xrightarrow{k_m'} 2V^{III}V^{IV}(ttha) + O_2^{2-} \quad (14)$$

$$O_2^{2-} + 2V_2O(ttha)^{2-} \xrightarrow{4H^+} 2V^{III}V^{IV}(ttha) + 2H_2O \quad (15)$$

$$\text{net: } 4V_2O(ttha)^{2-} + O_2 \xrightarrow{4H^+} 4V^{III}V^{IV}(ttha) + 2H_2O \quad (16)$$

$$\text{rate} = -\frac{d[V_2O(ttha)^{2-}]}{dt} = \frac{d[V^{III}V^{IV}(ttha)]}{dt} = 4k_m'[V_2O(ttha)^{2-}][O_2] \quad (17)$$

with enzyme

$$2V_2O(ttha)^{2-} + O_2 \xrightarrow{k_m'} 2V^{III}V^{IV}(ttha) + O_2^{2-} \quad (14)$$

$$O_2^{2-} + 2H^+ \xrightarrow{CAT} H_2O + {}^1/_2O_2 \quad (18)$$

$$\text{rate} = -\frac{d[V_2O(ttha)^{2-}]}{dt} = \frac{d[V^{III}V^{IV}(ttha)]}{dt} = 2k_m'[V_2O(ttha)^{2-}][O_2] \quad (19)$$

The reaction would be expected to be twice as fast without the enzyme as it is with the enzyme present. The reaction rate was not significantly affected by the addition of catalase at 7.08×10^{-6} M. Catalase disproportionates H_2O_2 with $k = 1.7 \times 10^7$ M^{-1} s^{-1}.[30] On the same solution of $V_2O(ttha)^{2-}$, a rate of 0.12 s^{-1} was seen without the enzyme and a rate of 0.15 s^{-1} was seen when the enzyme was present. $V_2O(ttha)^{2-}$ would have to reduce H_2O_2 at 5.1×10^5 M^{-1} s^{-1} if a 50% kinetic split were to be achieved in competition with catalase. Since $K_{H_2O_2}$ measured directly for the $V_2O(ttha)^{2-}/H_2O_2$ reaction is only 307 M^{-1} s^{-1}, the $V_2O(ttha)^{2-}$ could not react with any H_2O_2, produced by an outer-sphere path, rapidly enough to compete with active catalase. Since no rate suppression was observed, H_2O_2 could not be produced by the reaction if catalase could be shown to be in its active form.

The catalase was shown to be catalytically active. After an experiment was concluded in which the effect of catalase on the reaction of $V_2O(ttha)^{2-}$ and O_2 was studied, the stopped-flow instrument was thoroughly rinsed. This consisted of rinsing over 150 mL of deionized water and then 50 mL of deoxygenated, deionized water through the system. Then a fresh aliquot of the same stock $V_2O(ttha)^{2-}$ solution was loaded into one barrel and a peroxide solution was loaded into the other. When these reagents were mixed, the measured rate was about twice as fast as the rate seen for the $V_2O(ttha)^{2-}/O_2$ reaction. A repeat mix from the drive syringes produced a rate that was slower, and by the time a third mix was taken from the drive syringe reagent pool, the rate was about the same as that of the $V_2O(ttha)^{2-}/O_2$ reaction. (The O_2 was produced by destruction of H_2O_2 by catalase.) The small amount of residual catalase left in the stopped-flow instrument was enough to destroy part of the peroxide in the drive syringe. After the stopped-flow apparatus had been washed with acid to destroy the residual catalase, the $V_2O(ttha)^{2-}/O_2^{2-}$ reaction was repeated. The $V_2O(ttha)^{2-}$ solution used on this day had a reaction rate of 210 M^{-1} s^{-1} with O_2 and a rate of 307 M^{-1} s^{-1} with H_2O_2. Radical-trapping studies described below unambiguously confirm that no H_2O_2 is produced by outer-sphere electron-transfer processes in support of the enzyme studies.

Scheme I

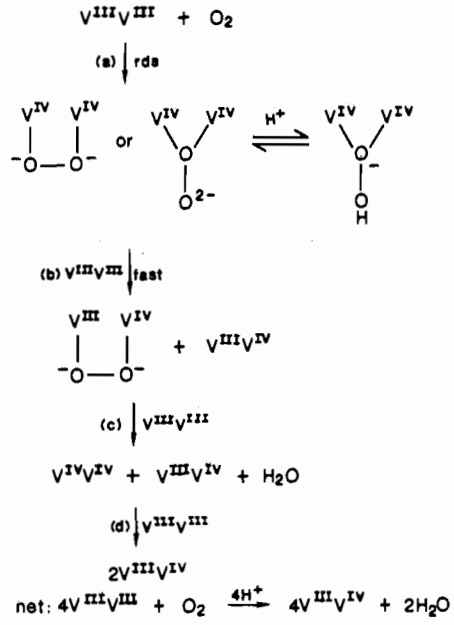

An alternate trap for either free H_2O_2 or O_2^- was carried out with $TiO(edta)^{2-}$ as the trapping agent.[22,23] No $Ti(O_2)(edta)^{2-}$ was formed during the course of the $V_2O(ttha)^{2-}/O_2$ reaction when $TiO(edta)^{2-}$ was placed in the O_2 reagent barrel. Again the absence of either free H_2O_2 or O_2^- is indicated by these results in support of the enzyme studies.

Scheme I shows a possible mechanism involving a bound peroxide complex that is not affected by the presence of CAT or $TiO(edta)^{2-}$ (rds = rate-determining step). Step d of this mechanism involves the reaction of a V(IV) dimer with a V(III) dimer, for which $k^{-cr} \cong 1.9 \times 10^{-2}$ M^{-1} s^{-1} (see the previous discussion). The reaction of $V_2O(ttha)^{2-}$ and O_2 has a rate of about 170 M^{-1} s^{-1} at a similar pH. Since the reaction between $V^{III}{}_2O(ttha)^{2-}$ and $V^{IV}{}_2(ttha)$ is 4 orders of magnitude slower than the rate-determining step of the $V_2O(ttha)^{2-}/O_2$ reaction, this mechanism may also be eliminated. If the reaction sequence in Scheme I were to stop at step c, the amount of $[V^{III},V^{III}]$ recovered in pulse experiments described below would yield only a maximum of 33% recovery of the $[V^{III},V^{III}]$ ion. Yields in excess of 33% are obtained. Therefore, the reactions shown in Scheme I cannot explain the data.

Spin-Trapping Studies of Species in the Reduction of O_2 and H_2O_2 by $V_2O(ttha)^{2-}$. Spin-trapping studies using DMPO or PBN[1b] have proven useful as a diagnostic tool in the detection of intermediates that are produced in O_2 and H_2O_2 reductions. The technique has been reviewed by Janzen[31] and by Evans.[32] Particularly, DMPO is useful in differentiation between O_2^- and HO•, which is formed in the one-electron-reduction sequence of O_2 and H_2O_2, respectively. The general case for DMPO and free radical, R•, is shown in eq 20. When R• = HO•, the DMPO radical adduct exhibits a four-line 1:2:2:1 intensity pattern in its ESR spectrum near $g = 2$; the coupling constants of the unpaired electron for N and the α-hydrogen are observed to be $a_N = 15.0$

(30) Chance, B. *Investigation of Rates and Mechanisms of Reactions*; Interscience: New York, 1963; Part II. Ochiai, E. I. *Bioinorganic Chemistry, An Introduction*; Allyn and Bacon: Boston, 1977; pp 143–147.

(31) Janzen, E. G. *Acc. Chem. Res.* **1971**, *4*, 31–40.
(32) Evans, C. A. *Aldrichim. Acta* **1979**, *12*, 23–30.

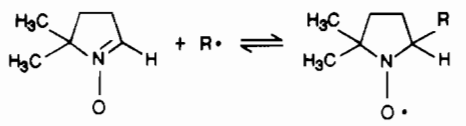

(20)

G (H_2O), 15.3 G (C_6H_6) and a_H = 15.0 G (H_2O), 15.3 G (C_6H_6).[33,34] If R = $HO_2^{\bullet}$ (protonated O_2^-), a six-line pattern, all lines of equal intensity, is obtained with a_N = 14.3 G and a_H = 11.7 G in C_6H_6.[34] In this way O_2^- may be differentiated from $HO^{\bullet}$ by the ESR spectrum of the trapped DMPO adduct. In aqueous solution, the dismutation of O_2^- into O_2 and H_2O_2 (eq 21) must be considered; O_2^-, itself, is trapped only at low con-

$$2O_2^- + 2H_3O^+ \rightarrow O_2 + H_2O_2 + 2H_2O \qquad (21)$$

centrations where the second-order dismutation is retarded. In the presence of reducing agents for O_2 in aqueous solution, one may actually trap the $HO^{\bullet}$ adduct from the reduction of H_2O_2 ($H_2O_2 + e^- \rightarrow HO^{\bullet} + OH^-$) in a secondary event as, for example, in the outer-sphere reduction of O_2 by $Ru(NH_3)_6^{2+}$.[33,35] Because both O_2^- and $HO^{\bullet}$ are very reactive radicals, it is often useful to trap secondary, longer lived radicals by reactions with alcohol scavengers such as ethanol[31-33] as shown in eq 22. The car-

$$HO^{\bullet} + CH_3CH_2OH \rightarrow CH_3CHOH + H_2O \qquad (22)$$

bon-centered radicals are reducing radicals and are very much less prone to reduction by the metal ion reductants than are O_2^- or $HO^{\bullet}$. The resultant CH_3CHOH radical may then be intercepted by DMPO or PBN in eq 20. The $R^{\bullet}$ adducts of DMPO or PBN have different coupling constants due to different inductive effects in the radical adduct compared to O_2H or $OH^{\bullet}$. The literature values for the ESR parameters of the CH_3CHOH trapped adduct (six-line equal-intensity pattern) are a_N = 16.2 G and a_H = 23.2 G for DMPO.[33]

The spin-trapping procedure has received use in characterizing the products of metal ion/peroxide redox reactions.[33,36-38] As these reactions are often relevant to biochemistry, the technique has been applied to biological redox reactions such as the electron transport in spinach chloroplasts.[39] The production of O_2^- and $HO^{\bullet}$ in the O_2-mediated oxidation of the ferrous form of the bleomycin antitumor drugs is of similar interest. The use of spin-trapping agents, including DMPO and PBN, has been reviewed for the bleomycin model drugs.[40] We have recently studied a series of O_2 and H_2O_2 reductions that are known to produce O_2^- and $HO^{\bullet}$ only by outer-sphere electron-transfer steps and some that are certain to proceed via coordinated O_2^-, as in the Ti(edta)$(H_2O)^-/O_2$ reaction.[41,42] The results of these studies with DMPO and PBN[41] show that $HO^{\bullet}$ is readily trapped, either by direct means or with alcohol mediators, when H_2O_2 is reduced by one-electron steps. When O_2^- is generated in an outer-sphere process, either HO_2, when it is formed at sufficiently low concentration, or its $HO^{\bullet}$ decay product via eq 21, when O_2^- production is high, may be detected by using DMPO. When O_2^- is produced by inner-sphere oxidation of metal centers, no radicals

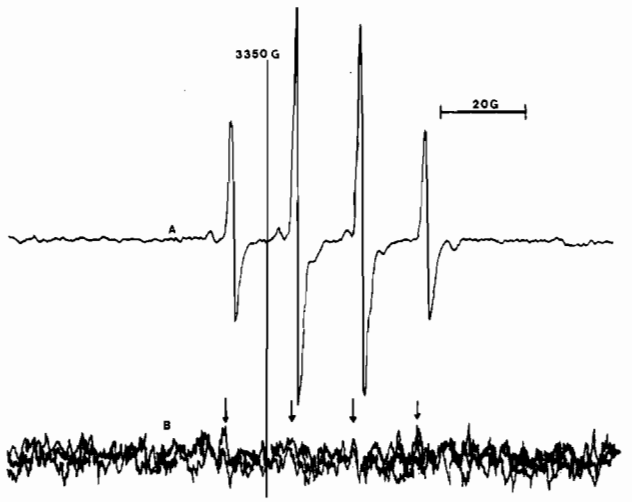

Figure 10. DMPO radical-trapping experiments with $V_2O(ttha)^{2-}$: (A) [DMPO] = 1.80 × 10^{-2} M, [H_2O_2] = 1.36 × 10^{-3} M, [$V_2O(ttha)^{2-}$] = 1.36 × 10^{-3} M; (B) [DMPO] = 2.25 × 10^{-2} M, [$V_2O(ttha)^{2-}$] = 4.5 × 10^{-4} M; O_2-saturated solution. All spectra were obtained at 9.405 GHz, 10-mW power, and 0.80-G modulation amplitude; receiver gains (A) 6.3 × 10^3 and (B) 4.0 × 10^4; repetitive scans at 4.0 min.

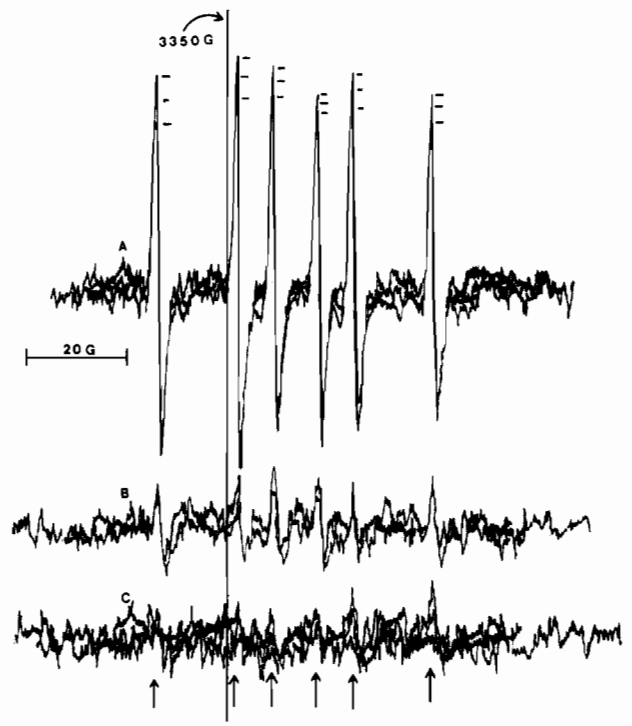

Figure 11. Ethanol-mediated DMPO radical-trapping experiments: (A) [DMPO] = 2.37 × 10^{-2} M, [$V_2O(ttha]^{2-}$] = 4.7 × 10^{-4} M, [H_2O_2] = 3.16 × 10^{-3} M, [C_2H_5OH] = 1.81 M; (B) [DMPO] = 1.80 × 10^{-2} M, [$V_2O(ttha)^{2-}$] = 4.0 × 10^{-4} M, [C_2H_5OH] = 1.56 M, O_2-saturated and Ar-purged; (C) [DMPO] = 1.80 × 10^{-2} M, [$V_2O(ttha)^{2-}$] = 4.0 × 10^{-4} M, [C_2H_5OH] = 1.56 M, O_2-saturated. All spectra were obtained at 9.405 GHz, 10-mW power, and 0.80-G modulation amplitude; receiver gains 4.0 × 10^4; repetitive scans at 4.0 min.

with ESR parameters the same as those of free O_2^- or $HO^{\bullet}$ are detectable.[41] These prior studies serve as a basis for diagnosis of intermediates in reactions of O_2 and H_2O_2.

DMPO and PBN radical-trapping experiments were performed as described in the Experimental Section for the $V_2O(ttha)^{2-}/O_2$ and $V_2O(ttha)^{2-}/H_2O_2$ reactions at [$V_2O(ttha)^{2-}$] = (1.4–0.14) × 10^{-3} M. Both systems were characterized in the absence and presence of ethanol as a potential mediator via CH_3CHOH in the detection process. The results of the DMPO experiments are shown in Figures 10 and 11; equivalent results were obtained with the PBN trap, confirming the presented results. The V_2O-

(33) Johnson, C. R.; Shepherd, R. E. In *Mechanistic Aspects of Inorganic Chemistry*; Rorabacher, D. B., Endicott, J. F., Eds.; *ACS Symposium Series* 198; American Chemical Society: Washington, DC, 1982.
(34) Janzen, E. G.; Liu, F. *J. Magn. Res.* **1973**, *19*, 510.
(35) Stanbury, D. M.; Haas, O.; Taube, H. *Inorg. Chem.* **1980**, *19*, 518–524.
(36) Gilbert, B. C.; Norman, R. O. C.; Sealy, R. C. *J. Chem. Soc., Perkin Trans. 2* **1973**, 2174–2180.
(37) Harbour, J. R.; Chow, V.; Bolton, J. R. *Can. J. Chem.* **1974**, *52*, 3549–3533.
(38) Kremer, M. L. *Isr. J. Chem.* **1971**, *9*, 321–327.
(39) Harbour, J. R.; Bolton, J. R. *Biochem. Biophys. Res. Commun.* **1975**, *64*, 803–807.
(40) Suguria, Y.; Takita, T.; Umezawa, H. *Met. Ions Biol. Syst.* **1985**, *19*, 81–108.
(41) Myser, T. K.; Johnson, C. R.; Shepherd, R. E., to be submitted for publication in *J. Am. Chem. Soc.*
(42) Kristine, F.; Shepherd, R. E.; Siddiqui, S. *Inorg. Chem.* **1981**, *20*, 2571–2579.
(43) The term "sided molecule" refers to the fact that the oxo-bridged $V_2O(ttha)^{2-}$ has a surface with the hydrophilic region about the metal centers and a more protected, hydrophobic region defined by the ligand backbone structure.

$(ttha)^{2-}/H_2O_2$ reaction clearly shows the HO• radical adduct of DMPO is detected at high intensity (Figure 10A). The coupling constants $a_N = a_H = 15.0$ G and the 1:2:2:1 pattern is diagnostic of the HO• adduct. The radical that was trapped was independent of the ratio $[H_2O_2]:[V_2O(ttha)^{2-}]$. When O_2 is used to oxidize $V_2O(ttha)^{2-}$, only a very weak signal, barely detectable above the noise at the highest tolerable receiver gain, is found (Figure 10B). The arrows show the predicted location of the four-line pattern. The result displayed in Figure 10B represents the optimum case, as higher and lower $[V_2O(ttha)^{2-}]_i$ yielded no discernible signal.

These results imply that very little free O_2^- is generated in the $V_2O(ttha)^{2-}/O_2$ system. This study substantiates the absence of the effect of the SOD enzyme on the kinetics of this process.

An effort was made to amplify the trapping step by use of ethanol at ca. 1.5 M as an intermediate scavenger. When HO• is generated with H_2O_2 as the added oxidant, the presence of ethanol results in the trapping of the CH_3CHOH mediator radical by DMPO (see Figure 11A). The ESR parameters of $a_N = 16.0$ G and $a_H = 23.2$ G are those of the authentic CH_3CHOH adduct of DMPO.[33] The radical spectrum slowly decreases during the repetitive 4.0-min scans, which precludes signal averaging as a method to enhance weaker signals of the O_2 activated system. The total time to fill the ESR cell and to initiate a spectral sweep is about 6 min when Ar purging preceded filling of the ESR quartz flat cell and 3.0 min if the Ar purging step to remove excess O_2 was omitted. A slight additional paramagnetic broadening of the organic radical species occurs with O_2 present (compare Figure 11C with the Ar-purged sample shown in Figure 11B). However, in either case only a very weak signal of the trapped CH_3CHOH adduct is detected with O_2 as the oxidant for $V_2O(ttha)^{2-}$. On the basis of the relative intensity found in Figure 11A and those in Figure 11B,c it is calculated that $\leq 12\%$ of the $V_2O(ttha)^{2-}/O_2$ reaction may proceed by outer-sphere production of O_2^-. Data from the direct trapping of HO• via H_2O_2 reduction (Figure 10A) and $2O_2^- \rightarrow H_2O_2 \rightarrow$ HO• (Figure 10B) gives a supporting value that $\leq 7\%$ of the $V_2O(ttha)^{2-}/O_2$ reaction involves outer-sphere O_2^- production. This result can only specify the upper limit of O_2^- production by an outer-sphere pathway. It is conceivable that some of the detected yield could originate via dissociation of O_2^- formed during an inner-sphere process, or it may be produced from contamination sources such as trace Cu(I) and Fe(II) in the reagents or, in the case of the alcohol-mediated system, from H atom abstraction by the coordinated O_2^- moiety.

One should note that had outer-sphere H_2O_2 been produced as an intermediate in the $V_2O(ttha)^{2-}/O_2$ reaction, the HO• adduct of DMPO would be detected at levels at least one-third as large as the signals shown in Figures 10A and 11A. Since no such signal is detectable in either case, no H_2O_2 can be formed in outer-sphere steps for the $V_2O(ttha)^{2-}/O_2$ reaction. This is the same conclusion as reached by the absence of a kinetic influence of catalase on the same process.

Even if O_2^- were produced by an outer-sphere reaction and it were further reduced by $V_2O(ttha)^{2-}$ so rapidly that no O_2^- were available for detection, the H_2O_2 formed by sequential one-electron reductions would also yield at least one-third the recorded signals for Figures 10A and 11A. *Thus free O_2^- and H_2O_2 cannot be the intermediates in the $V_2O(ttha)^{2-}/O_2$ reaction.* Neither the stoichiometry nor the rate law in the physiological pH range was changed by the presence of added superoxide dismutase (SOD) or catalase (CAT). Therefore, *any mechanism forming free O_2^- or H_2O_2 is eliminated* by the enzyme and radical-trapping-agent tests. The alternate conclusion which must be drawn is that the $V_2O(ttha)^{2-}/O_2$ reaction *proceeds $\geq$Ca. 90% by inner-sphere coordination of O_2* in forming a $[V^{III},V^{IV}O_2^-]$ complex. The chemistry of this species is described in a subsequent section.

The best mechanism compatible with all our data and $[V^{III},V^{IV}]$ as the product is an initial 1e rate-limiting inner-sphere reduction of O_2 followed by rapid reduction of coordinated O_2^- to H_2O (Scheme II). Thus, coordinated O_2^- remains inaccessible to SOD enzyme and is reduced to H_2O without release of O_2^{2-}.

In Scheme II $k_1 = Kk_H$. If K is as great as 10^2 M^{-1}, an upper realistic limit for protonation at a carboxylate or perhaps the oxo bridge, the amount of $V_2O(Httha):V_2O(ttha)^{2-}$ is still $\sim 10^{-7}$:1 at pH 7.0. Thus, the species would go undetected spectrophotometrically, yet $V_2O(Httha)^-$ would carry 14% of the rate. With this assumption on the magnitude of K, k_H then equals 2.08×10^6 M^{-1} s^{-1}. Comparison of the reaction of $V_2O(ttha)^{2-}$ and $V_2O(Httha)^-$ with O_2 then reveals the proton path with a relative rate advantage of about 1.5×10^4. This is within a factor of 10 of the relative kinetic advantage of the proton-assisted path to the unassisted path in the $[V^{III},V^{IV}]$ cross reaction when protonation was assumed at the carboxylate, which would open a coordination site for O_2 on $V_2O(ttha)^{2-}$. The site of protonation is most likely near the V(III) center, and protonation yields a similar structural reorganizational advantage in both cases.

Scheme II

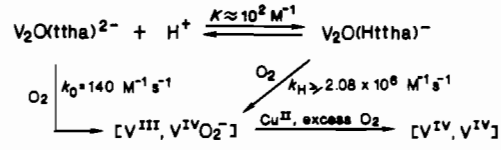

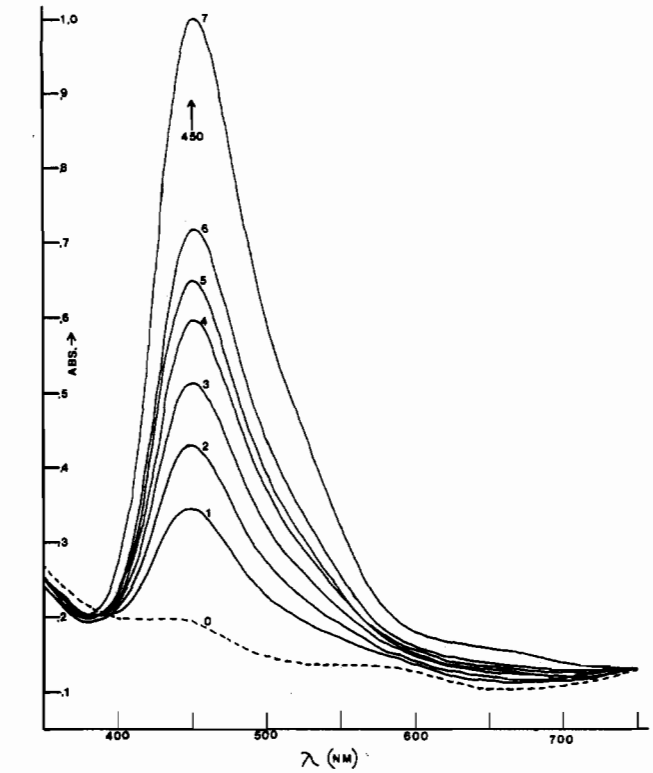

Figure 12. Re-formation of the $[V^{III},V^{III}]$ complex from the superoxo intermediate complex $[V^{III},V^{IV}O_2^-]$ ($[V^{III},V^{III}]_{int} = 1.5 \times 10^{-3}$ M, μ = 0.01).

Fate of the $[V^{III},V^{IV}O_2^-]$ Complex. In the presence of excess O_2 the ultimate product of the $O_2/V_2O(ttha)^{2-}$ reaction was found to be $[V^{IV},V^{IV}]$ as indicated in Scheme II. It was shown that the system could be intercepted at the $[V^{III},V^{IV}]$ oxidation-state level if excess O_2 were purged from the solution immediately after the original rapid decay of the $[V^{III},V^{III}]$ spectrum upon mixing with O_2. Spectra taken of the Ar-purged solution were shown to slowly regenerate up to 50% of the initial $[V^{III},V^{III}]$ complex. A typical example is shown in Figure 12. The value of A_∞ at 450 nm was used to construct a second-order kinetic plot (Figure 13). The rate constant for the regeneration of $[V^{III},V^{III}]$ was observed to be the same as found from the cross-reaction studies in which $[V^{III},V^{IV}]$ was prepared kinetically from equimolar amounts of V(III), V(IV), $ttha^{6-}$.

A second check of the nature of the recovery reaction forming $[V^{III},V^{III}]$ was made by using $Na_6Co_2(CN)_{10}\cdot 4H_2O$ as a possible scavenger for O_2. If the $[V^{III},V^{IV}O_2^-]$ intermediate were to reversibly dissociate O_2 to regenerate the $[V^{III},V^{III}]$ complex after the Ar purge, the liberated O_2 would be available to oxidize

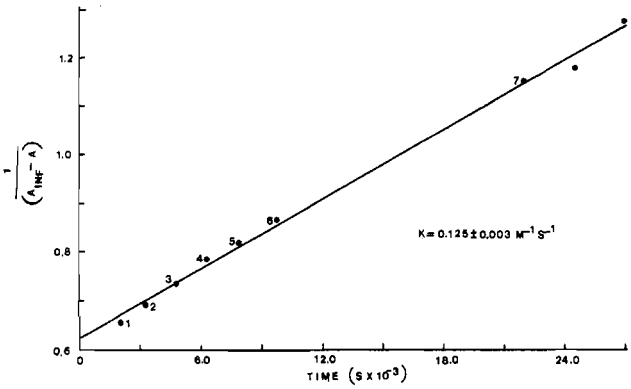

Figure 13. Second-order plot of the re-formation of the $[V^{III},V^{III}]$ complex (same conditions as Figure 12).

$Co(CN)_5^{3-}$, forming either $(CN)_5CoOH_2^{2-}$ or the peroxo-bridged complex $(CN)_5Co(O_2)Co(CN)_5^{6-}$.[25] No evidence for the formation of the oxidized Co(III) complexes could be obtained. $[Co_2(CN)_6^{6-}]_0$:$[V^{III},V^{III}]_0$ was set at 1:26 in order to keep spectral features of the cobalt complexes on scale and to assure that even as much as 5% dissociation of O_2 would consume all of the $Co(CN)_5^{3-}$ in the sample. In a typical experiment the $[V^{III},V^{IV}O_2^-]$ intermediate was prepared by admission of O_2 to a solution of $[V^{III},V^{III}]$. The excess O_2 was purged for 15 min, and then the $Co(CN)_5^{3-}$ solution was added and the solution was allowed to sit quietly under Ar for 4 h while spectra were taken. In a blank experiment the $Co(CN)_5^{3-}$ solution was shown to be rapidly oxidized by O_2 as detected by the loss of $Co(CN)_5^{3-}$ bands at 280 and 613 nm and the appearance of a new band at 375 nm attributed to the final $(CN)_5CoOH_2^{2-}$ product.[25] No appearance of the 375-nm band was detected in the $[V^{III},V^{IV}]/Co(CN)_5^{3-}$ solution. Therefore, O_2 dissociation from $[V^{III},V^{IV}O_2^-]$ is not the direct source of the regeneration of $[V^{III},V^{III}]$. The percent recovery of $[V^{III},V^{III}]$ was variable from 16 to 50% from run to run. However, the rates of recovery were within experimental error of the same value.

Two chemical schemes, given in Schemes III and IV, are able to account for the slow reappearance of $[V^{III},V^{III}]$. Scheme III involves the rapid reduction of the coordinated O_2^- moiety by 3 mol of $V_2O(ttha)^{2-}$. For simplicity only the oxidation states of the various vanadium species are shown; the initial concentration is shown as a_0 to follow the product yields.

Scheme III

$$\underset{a_0/4}{(III,III)} + O_2 \rightarrow \underset{a_0/4}{[(III,IV)O_2^-]} \quad (23)$$

$$\underset{a_0/4}{[(III,IV)O_2^-]} + \underset{3a_0/4}{3(III,III)} \xrightarrow{fast} \underset{a_0}{4(III,IV)} + 2H_2O \quad (24)$$

$$\underset{a_0}{2(III,IV)} \xrightarrow[k = 0.125\ M^{-1}\ s^{-1}]{rds} \underset{a_0/2}{(III,III)} + \underset{a_0/2}{(IV,IV)} \quad (25)$$

$$(III,IV) \xrightarrow{Cu^{2+}/O_2} (IV,IV) \quad (26)$$

The alternate mechanistic possibility involves the spontaneous dismutation of the $[V^{III},V^{IV}O_2^-]$ species via a coordinated peroxo intermediate as shown in Scheme IV.

Scheme IV

$$\underset{a_0}{2[(III,IV)O_2^-]} \rightarrow \underset{a_0/2}{(III,IV)} + \underset{a_0/2}{[(III,IV)O_2^{2-}]} + O_2 \quad (27)$$

$$\underset{a_0/2}{2[(III,IV)O_2^{2-}]} \xrightarrow{fast} \underset{a_0/2}{2(III,IV)} + O_2 + 2H_2O \quad (28)$$

$$\underset{a_0}{2(III,IV)} \xrightarrow[k = 0.125M^{-1}\ s^{-1}]{rds} \underset{a_0/2}{(III,III)} + \underset{a^0/2}{(IV,IV)} \quad (25)$$

$$(III,IV) \xrightarrow{Cu^{2+}/O_2} (IV,IV) \quad (26)$$

If rapid reduction of the coordinated O_2^- complex (Scheme III) were the proper pathway, no dioxygen-containing species would be present at the time of the $Co(CN)_5^{3-}$ addition. No release of O_2 would be involved. The cross reaction (eq 25) would regenerate the isovalent pair of products with a maximum predicted yield of 50% of $V_2O(ttha)^{2-}$. Variability in the purging efficiency and the amount of catalytic contaminants would lower the observed yield below 50% due to the competitive reaction shown in eq 26, which is slower than steps 23 and 24, but faster than step 25.

A 50% maximum recovery of $[V^{III},V^{III}]$ would be predicted by the sequential dismutation of the superoxo and peroxo intermediates as given in Scheme IV. As long as steps 27 and 28 are rapid and complete within the 15-min purging time of the $Co(CN)_5^{3-}$ experiment, no released O_2 will be trapped by $Co(CN)_5^{3-}$. Therefore, Schemes III and IV are kinetically indistinguishable by the $Co(CN)_5^{3-}$ experiment, and the only conclusion that can be drawn from it is that O_2 is not released during events that lead directly to recovery of $V_2O(ttha)^{2-}$ (e.g. step 25).

Several experiments were attempted in which O_2 was the limiting reagent. The band at 450 nm was completely bleached at 2.6:1 $[V^{III},V^{III}]_0$:$[O_2]$. The complete consumption of the $[V^{III},V^{III}]$ ion infers that both the superoxo and peroxo intermediates are reducible by $[V^{III},V^{III}]$ (eq 29 and 30). This lends support to Scheme III as the more probable pathway.

$$[(III,IV)O_2^-] + (III,III) \rightarrow (III,IV) + [(III,IV)O_2^{2-}] \quad (29)$$

$$[(III,IV)O_2^{2-}] + (III,III) \rightarrow 2(III,IV) + 2H_2O \quad (30)$$

Open-Chain Form in Solution. It was of concern during these studies to know if any significant amount of the open-chain form (structure **1A**) might be at equilibrium with the closed form (structure **1B**) at pH ~7. The open-chain form of $[V^{III},V^{III}]$ was prepared by using a 2:1 mixture of VCl_3 and $ttha^{6-}$ and adjusting the pH to about 3 such that no charge-transfer band at 450 nm (characteristic of $V_2O(ttha)^{2-}$) was observed. O_2 was bubbled through the open-chain $[V^{III},V^{III}]$ solution for 1 h. Recall that the closed form, $V_2O(ttha)^{2-}$, reacts completely with O_2 in 10 s. After O_2 was bubbled for 1 h, the O_2 was purged with Ar and the pH adjusted to about 7. A total of 83% of the V(III) was recovered as $V_2O(ttha)^{2-}$. Therefore, the open-chain form of $[V^{III},V^{III}]$ must oxidize very slowly with O_2, similar to the result for the monomeric equivalent $V(hedta)(H_2O)$. The re-formation of the bridged form at pH ≅7 was complete in less than 2 min. Therefore, closure of the bridge must be rapid with $k \geq 5.8 \times 10^{-2}\ s^{-1}$. If there were a substantial amount of the open-chain form at pH ≅7, then the recovery step yielding $[V^{III},V^{III}]$ might have been attributed to a slow re-formation of the bridged $V_2O(ttha)^{2-}$ (structure **1B**) rather than a cross-electron-transfer step. This possibility is completely ruled out by the rapid formation of the bridged form at pH ≅7, as well as the second-order nature of the re-formation of $[V^{III},V^{III}]$.

Summary

$ttha^{6-}$ binds V(III) and V(IV) in a series of binuclear complexes including the isovalent species $[V^{III},V^{III}]$ and $[V^{IV},V^{IV}]$ and the mixed-oxidation-state $[V^{III},V^{IV}]$ complex. Both isovalent ions are apparently bridged in solution by the oxo group. The isovalent pair of ions are modestly more stable than $[V^{III},V^{IV}]$. The value of the comproportation constant in the formation of $[V^{III},V^{IV}]$ is only 0.15. Therefore, the latter executes a cross-electron-transfer reaction by relatively slow proton-independent and -dependent paths with rate constants of $5.08 \times 10^{-2}\ M^{-1}\ s^{-1}$ and $6.53 \times 10^5\ M^{-2}\ s^{-1}$, respectively. The slow nature of the electron transfer originates in the different coordination numbers required by the V(III) and V(IV) sites.

$[V^{III},V^{III}] = V_2O(ttha)^{2-}$ reacts rapidly with O_2, binding in the inner sphere as a superoxo complex, $[V^{III},V^{IV}O_2^-]$. The presence of two metal sites appears to be important in generating a stabilized superoxo intermediate as the oxidation of the open-chain form of $[V^{III},V^{III}]$ or of $V(hedta)(H_2O)$ is very slow. Therefore, the superoxo group is probably bridging between V(III) and V(IV) sites. In the presence of excess O_2, the final product is the

$[V^{IV},V^{IV}]$ complex. However, a rapid purge of excess O_2 following the initial binding in the $[V^{III}, V^{IV} O_2^-]$ intermediate allows the observation of a slow re-formation of some $V_2O(ttha)^{2-}$. In the process a pool of the $[V^{III},V^{IV}]$ complex is created either by reduction of all $[V^{III},V^{IV}O_2^-]$ species to $[V^{III},V^{IV}]$ or by dismutation of the superoxo complex into a peroxo complex and finally to $[V^{III},V^{IV}]$. The cross-electron-transfer reaction then regenerates up to 50% of $V_2O(ttha)^{2-}$.

Acknowledgment. We express appreciation for support of this study under National Science Foundation Grant Nos. CHE802183 and CHE8417751.

Contribution from the Department of Chemistry,
University of Pittsburgh, Pittsburgh, Pennsylvania 15260

Formation of $[(CN)_5Ru^{II}–CN–Ru^{III}(CN)_5]^{6-}$ by Chemical Oxidation, Electrochemical Oxidation, and Photooxidation of $Ru(CN)_6^{4-}$

Kamal Z. Ismail, M. S. Tunuli, and Stephen G. Weber*

Received September 12, 1985

Electron transfer to a ligand field excited state of tris(glycinato)cobalt(III) by hexacyanoruthenium(II) was observed in pH 5 acetate-buffered aqueous solution. A product of the reaction is a species that has an intervalence transfer band at 9.1×10^3 cm^{-1} (1094 nm) with a molar absorptivity of about 7×10^3 M^{-1} cm^{-1}. The same spectroscopic band results from chemical oxidation (H_2O_2, Ce^{4+}), anodic oxidation (Pt electrode), and excited-state electron transfer to tris(2,2'-bipyridine)ruthenium(II). Steady-state analysis of the kinetics of the reaction leads to an estimation of the lifetime of the excited state of tris(glycinato)cobalt(III) as 23 ± 4 ns. The most likely species responsible for the infrared band is the cyanide-bridged dimer $[(CN)_5Ru^{II}–CN–Ru^{III}(CN)_5]^{6-}$. The kinetics of its formation from hexacyanoruthenium(II) and -(III) are rapid (second-order rate constant $\sim 1 \times 10^4$ M^{-1} s^{-1}) in contrast to recent observations on nonphotochemical reactions of hexacyanoruthenium(III).

Introduction

Our laboratory is interested in the development of photoelectrochemistry as an analytical tool.[1,2] This technique uses an EC catalytic mechanism of electron transfer from an electrode to an acceptor (quencher) in solution via a photoexcited $Ru(bpy)_3^{2+}$.[2-9] In the course of investigations into the suitability of tris(amino acid) complexes of Co(III) as quenchers of $Ru(bpy)_3^{2+*}$ and of $Ru(CN)_6^{4-}$ as an electron-transfer mediator between $Ru(bpy)_3^{3+}$ and a cathode, we have found evidence that a nonluminescent ligand field excited state of tris(glycinato)cobalt(III), $Co(gly)_3$, undergoes electron transfer with $Ru(CN)_6^{4-}$. Our observations are particularly significant in view of the fact that the bimolecular electron-transfer photochemistry of nonluminescent excited states is known only in a few cases[10-13] and the methods for studying these reactions are difficult. The findings and methodology described below, though not always applicable, have the potential to allow investigations of other nonluminescent states. Furthermore, the result of photolysis is a spectroscopic band with the characteristics[14] of an intervalence charge-transfer band (ν_{IT} = 9.1×10^3 cm^{-1}). The simplest species that could give rise to this feature is the cyanide-bridged binuclear complex $[(CN)_5Ru^{II}–CN–Ru^{III}(CN)_5]^{6-}$ (I).

Experimental Section

Materials. Preparation of $Co(gly)_3$ is described in ref 1. $Ru(CN)_6^{4-}$ (Alfa Products), NaCN (Fisher), and $Ru(bpy)_3^{2+}$ (G. F. Smith) were used as received. All solutions were prepared in 0.1 M acetate buffer, pH 5.00 ± 0.05, prepared in distilled–deionized water. $Ru(CN)_6^{3-}$ was prepared according to Crean and Schug.[15] $Ru(CN)_5OH_2^{3-}$ was prepared according to Johnson and Shepherd.[16]

Methods. (a) Electrochemistry. Cyclic voltammetric experiments were performed by using a BAS CV-1A potentiostat and data were recorded on an X-Y recorder (Houston Instruments). Constant-potential electrolysis of $Ru(CN)_6^{4-}$ was carried out by using a PAR 173 potentiostat–galvanostat. Absorbance was determined with an IBM 9420 UV–vis spectrophotometer. The electrochemical cells used were either a spectrophotometer cuvette or a vial with a conventional three-electrode configuration. An Ag/AgCl (3 M NaCl) reference electrode and a Pt-wire auxiliary electrode were used. The working electrode was a glassy-carbon button (0.07 cm^2). The working electrode in the spectroelectrochemical experiment was a Pt wire. All experiments were carried out in 0.1 M acetate, pH 5.00 ± 0.05, electrolyte.

(b) Steady-State Photolysis. A 2-mL aliquot of a given reaction mixture was continuously photolyzed by using the 441.6-nm beam of a nominally 40-mW CW He–Cd laser. All solutions were continuously stirred during photolysis with a magnetic stirrer. The base-line-corrected difference (photolyzed minus unphotolyzed) absorption spectra were recorded on an IBM 9420 UV–vis spectrophotometer. Results shown in Figure 1 were recorded on a Cary-14 UV–vis–IR spectrophotometer. Incident light intensity was monitored on a Spectra Physics power meter (401 B). All experiments were carried out at ambient temperature, 22 ± 1 °C.

(c) Errors. All errors reported represent 95% confidence intervals determined from a linear least-squares treatment.

Results and Discussion

Quenching of the Nonluminescent Excited State of $Co(gly)_3$ and Formation of the Binuclear Complex. Irradiation of a solution of 1.0×10^{-3} M $Co(gly)_3$ in 0.1 M acetate, pH 5, buffer leads to no spectral change in a 10-min photolysis. Likewise a solution 1.0×10^{-2} M in $Ru(CN)_6^{4-}$ suffers no spectral change when photolyzed for 10 min. When these two solutions are mixed, either

(1) Weber, S. G.; Morgan, D. M.; Elbicki, J. M. *Clin. Chem. (Winston-Salem, N.C.)* **1983**, *29*, 1665.
(2) Elbicki, J. M.; Morgan, D. M.; Weber, S. G. *Anal. Chem.* **1985**, *57*, 1746.
(3) Gafney, H.; Adamson, A. W. *J. Am. Chem. Soc.* **1972**, *94*, 8238.
(4) Demas, J. N.; Adamson, A. W. *J. Am. Chem. Soc.* **1983**, *95*, 5159.
(5) Navon, G.; Sutin, N. *Inorg. Chem.* **1974**, *13*, 2159.
(6) Creutz, C.; Sutin, N. *Inorg. Chem.* **1976**, *15*, 496.
(7) Meyer, T. J. *Acc. Chem. Res.* **1978**, *11*, 94.
(8) Sutin, N. *J. Photochem.* **1979**, *10*, 19.
(9) Kalyansundaram, K. *Coord. Chem. Rev.* **1982**, *46*, 159.
(10) Kane-Maguire, N. A. P.; Langford, C. H. *J. Chem. Soc., Chem. Commun.* **1973**, 351.
(11) Langford, C. H.; Vuik, C. P. J.; Kane-Maguire, N. A. P. *Inorg. Nucl. Chem. Lett.* **1975**, *11*, 377.
(12) Langford, C. H.; Sasseville, R. L. *Can. J. Chem.* **1981**, *59*, 647.
(13) Indelli, M. T.; Cairoli, A.; Scandola, F. *J. Phys. Chem.* **1984**, *88*, 2685.
(14) Creutz, C. *Prog. Inorg. Chem.* **1982**, 30.
(15) Crean, F. M.; Schug, K. *Inorg. Chem.* **1984**, *23*, 853.
(16) Johnson, C. R.; Shepherd, R. E. *Inorg. Chem.* **1983**, *22*, 1117, 2439.

0020-1669/87/1326-1555$01.50/0